Macromolecules

Volume 24, Number 13 June 24, 1991

Reviews

A Chemical Approach to the Orbitals of Organic Polymers

Roald Hoffmann,* Christoph Janiak, and Christian Kollmar

Department of Chemistry and Materials Science Center, Cornell University, Ithaca, New York 14853-1301

Received September 8, 1990; Revised Manuscript Received January 8, 1991

ABSTRACT: The electronic structure of the prototypical unsaturated and saturated organic polymers polyacetylene and polyethylene is elucidated by a building-up process starting from a linear carbon chain, which is then kinked and finally has one or two hydrogen atoms attached to it. In this process the common features as well as the differences between polyacetylene and polyethylene (semiconductor vs large band gap insulator, unsaturation vs saturation) emerge in a natural way. The emphasis is on bringing together the essential concepts of solid-state physics and simple ideas of chemical bonding. Some topics of special interest, such as bond alternation and solitons in polyacetylene, are also discussed, in as simple and chemical manner as possible.

Synthetic organic polymers mark our time.[1] The most common such polymer, polyethylene (1), has an extremely

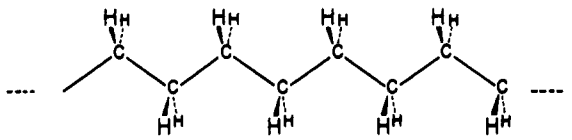

1

wide range of applications, responsible for its production volume of ~8 billion kilograms in the United States in 1989.[2] The interest in polyethylene and its derivatives derives not from its electronic properties—it is a large band gap insulator, generally colorless—but from its strength and mechanical properties.[3] These can be tuned over an impressive range, therefore the economic value of these synthetics. Even though the electronic properties of polyethylene appear to be less important than its mechanical ones, the underlying electronic structure determines all properties. The rational design of new synthetic polymers based on polyethylene must draw upon our knowledge of how the electrons move in this simplest polymer.

There are other polymers that have not yet found their way to practical application, but are interesting for different reasons. These are the conjugated polymers.[4] They also have a planar carbon backbone, but now an unsaturated one, one that provides for a conjugated π system consisting of p orbitals perpendicular to the plane of the backbone. This π system gives rise to interesting electronic properties,[5] thus attracting the attention of both physicists and chemists. For instance, it provides for localized elementary excitations known as solitons[6,7] and polarons[6,8] and nonlinear phenomena[9] of great interest to theorists. Some of these polymers become highly conducting on doping, as conducting as the best metals.[5,10] This makes them candidates for practical applications in the future; recently the mechanical strength of polyacetylene has reached an impressive magnitude.[11] At the moment, though, the conjugated polymers are interesting mainly for theoretical reasons.[12] In the way that reality and interest have of getting out of phase with each other, one suspects there are more people in academia working on conducting organic polymers (of no industrial value as yet) than there are working on the typical synthetic fibers and plastics (which represent a good fraction of the GNP of industrialized countries).

The simplest representative of the conjugated polymers is polyacetylene (2).[13] It is also the one that has been most thoroughly investigated, both theoretically and experimentally. The π system of this polymer localizes in alternating single and double bonds within the carbon backbone, due to a so-called Peierls distortion, a phenomenon we will discuss below. Undoped polyacetylene is a semiconductor with a large band gap of over 1.4 eV.[14]

0024-9297/91/2224-3725$02.50/0

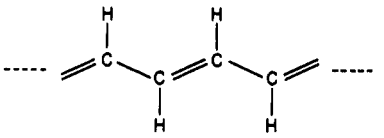

2

But it can be doped to be as conducting as copper.[10] The whole wealth of interesting electronic phenomena, which is so attractive to theorists, derives from the conjugated π system.[5]

Because polyethylene is both important and so simple in its structure, there have been many theoretical studies of it, at every level of sophistication.[15] These calculations are done not only because the unit cell is so small, but also because one needs the electronic structure to understand and interpret the experimental data on the valence and conduction band of polymers, derived from techniques such as UPS[18,21,22] XPS/ESCA[17,23,24] (ultraviolet, respectively, X-ray photoelectron spectroscopy/electron spectroscopy for chemical analysis), SEE[25-28] (secondary electron emission), EELS[29] (electron energy loss spectroscopy), photoconduction,[30,31] etc. On the side of polyacetylene, theoretical calculations of the band structure, some of which we have already mentioned, are still more abundant.[32]

What we want to do in this contribution is to put the electronic structure of these two polymers in their proper closely related perspective. Their striking similarities (C–C and C–H bonding) will emerge, as will their differences (saturation vs conjugation). A discussion of these polymers is also part of a pedagogic aim we have, which is to demystify solid-state theory, and to bring to chemists psychological comfort and confidence in dealing with bonding in extended systems.[33] Such confidence is necessary for chemists to enter as equal partners with physicists and engineers in the design of materials with unusual desired properties.

It must be said clearly at the outset that there is little original in this paper. The band structures of polyethylene and polyacetylene we present are available, from better calculations than ours, in the literature.[15,32] What is new is the pedagogical perspective, and the intent in every way possible to overcome the barriers of mind and jargon between chemical and physical perspectives of the same molecules.

Some further words on approximations and methodology may be in place here. Organic, organometallic, and inorganic polymers that crystallize in an extended chain form are ideal for both an experimental and a theoretical analysis if the *inter*chain interactions are weak. Such is the case for polyacetylene and polyethylene. This allows one in a good approximation to consider only a single isolated chain as determining the electronic structure of the bulk material.[19,34] One dimension is easier than two or three to think about; such single chains $(CH)_n$ and $(CH_2)_n$ are the subject of our paper.

While we will rely on qualitative arguments throughout this paper, we will support these by numerical experiments, that is calculations. On the computational level our discussion will be based on the extended Hückel method,[35] with which also the oldest band calculation of polyethylene was carried out.[36] The extended Hückel method is a simple, semiempirical molecular orbital (MO) method, yet quite successful in its agreement with experimental results for polyethylene.[17,18,20,30] We would like to stress, however, that our qualitative considerations are relevant to ab initio calculations as well.[37]

How to begin? An aufbau principle has served us well in understanding the structure of atoms, and fragment orbitals are a useful way to look at the bonding of complicated molecules.[38,39] It seems obvious that one should make use of the common feature of polyethylene and polyacetylene, namely their carbon backbone, if one wants to perceive their similarities. Accordingly, we begin with a simple linear carbon chain, in diagram 3. Finite

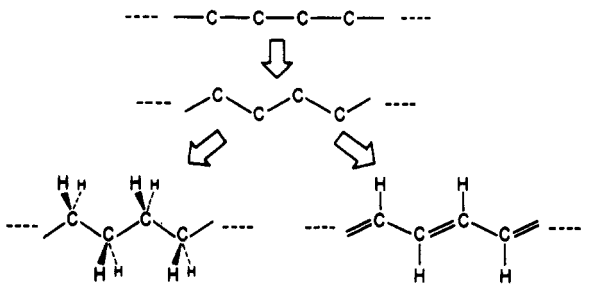

3

carbon chains, of course, have some interest on their own. Carbon clusters were first seen in arc discharges and the tails of comets.[40] Now they can be generated systematically and, for short chains, may have linear structures.[41] A synthesis of C_n chains of substantial length has been reported.[42]

To prepare the carbon chain for bonding in the polymers, this chain must be kinked. The addition of one or two hydrogens per carbon then "generates" polyacetylene or polyethylene. One of the very, very few advantages of theory over experiment is that molecules do not have to be made in the computer the way they are in the laboratory. So this theoretical construction bears no resemblance to any realistic synthesis of either polyethylene or polyacetylene. It is, however, a perfectly good way to get at the similarities and differences of our two polymers. But before we can embark on this theoretical construction we need to introduce the requisite theory.

The Tight-Binding Method

We need the orbitals of an infinite or long chain of carbon atoms. If N is the number of such atoms (N is large, perhaps approaching Avogadro's number) and each carbon has one 2s and three 2p orbitals, then the chains will have $4N$ atomic orbitals. From which we need to build $4N$ molecular orbitals. How to do this?

The procedure for accomplishing the task comes from solid-state physics and is called the tight-binding method. It is essentially the LCAO-MO method for a translationally periodic structure. Let us review the basics of a molecular orbital (MO) approach. For any system, molecular orbitals ψ_i are given by a linear combination of atomic orbitals ϕ_r:

$$\psi_i = \sum_r c_{ir}\phi_r \tag{1}$$

ψ_i represents the MO i with energy E_i, ϕ_r is an atomic orbital. The whole set $\{\phi_r\}$ of the AOs of the atoms composing the molecule constitutes the basis for any type of calculation within an LCAO scheme. One needs to determine the coefficients c_{ir} and the energies E_i.

Often certain constraints are placed on the coefficients c_{ir} by the symmetry of the molecule in question. It may even happen that the coefficients of the MOs are completely determined by symmetry and thus independent of the specific computational method applied. Consider, e.g., the hydrogen molecule. If we restrict our basis set to the

1s orbitals ϕ_1 and ϕ_2 of the two hydrogen atoms, we obtain two linear combinations for the MOs, a symmetric and an asymmetric one:

$$\psi_2 \sim \phi_1 - \phi_2 \qquad \psi_1 \sim \phi_1 + \phi_2 \tag{2}$$

Except for the unspecified normalization coefficient, which depends on the overlap integral of the nonorthogonal AOs, these MOs are completely determined by symmetry and therefore represent the only possible choice for the MOs. Another example, well-known to organic chemists, is the conjugated π system of benzene, the orbital pattern of which is also a consequence of the symmetry of the molecule.

Let us consider the most simple one-dimensional periodic array of atoms one can imagine, a linear chain of equally spaced hydrogen atoms (4). The repeat unit of this chain contains one H atom and is called the primitive unit cell. It is of length a.

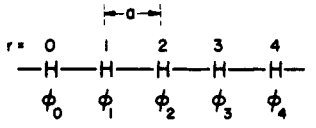

4

What do the electronic wave functions and energy values of this structure look like? If we use the LCAO approach, eq 1 can be applied, with the sum extending to infinity for an infinitely long chain and the basis set $\{\phi_r\}$ consisting of the H 1s orbitals. That linear hydrogen chain is highly symmetrical, though the symmetry in question, translational periodicity, sad to say, is not as familiar to chemists as it should be. The symmetry elements are the translational vectors given by integer multiples of the primitive vector connecting two neighboring H atoms in the chain. It turns out that the MOs are also completely determined by symmetry in that case. The symmetry-adapted wave functions are given by

$$\psi_k \sim \sum_{r=0}^{N-1} e^{ikra}\phi_r \tag{3}$$

These wave functions are the so-called Bloch sums. The analogy between eqs 1 and 3 is obvious. The index i of the coefficients in eq 1 has been replaced by the index k for reasons discussed below ($c_{kr} = e^{ikra}$). In order to tackle the mathematics of the problem, we have restricted ourselves to a large but finite number N of hydrogen atoms in the chain, which are labeled consecutively, as shown in 4. We then apply cyclic boundary conditions. This can be imagined as closing the finite chain to a ring. Thus, we demand that the wave function must have no discontinuity at the transition from atom $N-1$ to atom 0, the end positions of the former open chain. Atom 0 can now also be labeled N, because it follows atom $N-1$ in the ring. Thus

$$c_{kN} = c_{k0} \quad \text{or} \quad e^{ikNa} = 1 \tag{4}$$

This equation can be satisfied only if

$$kNa = j2\pi \quad \text{or} \quad k = j2\pi/Na \tag{5}$$

where j is an integer. k is quantized! Equation 5 shows us that the spacing between neighboring k values on the k axis is uniform, amounting to $2\pi/Na$, and therefore decreases as the number N of unit cells increases.

In analogy to the molecular case, the number of "MOs" (now called Bloch sums) must be equal to the number of atomic basis functions. Thus, we have N k values for N unit cells. Equation 5, of course, would allow more, but it may be seen from (3) that adding $2\pi/a$ to the k value does not change the coefficients of the wave function. It is therefore sufficient to restrict the k values to an interval of width $2\pi/a$. The standard choice is the interval ranging from $k = -\pi/a$ to $k = \pi/a$. This k range is called the first Brillouin zone of the one-dimensional lattice. Bits of the jargon of solid-state physics (also of diffraction theory) are now falling into place.

There are several meanings that can be assigned to k. First it is just a label distinguishing MOs. But it also distinguishes the irreducible representations of the translational group. A more physical interpretation is given by realizing that k is also a wave vector. The reason for this is that $(h/2\pi)k$ can be identified with the crystal momentum of an electron in a Bloch state, in accordance with the de Broglie relation, which connects the wave length and, thus, the wave vector of an electron with its momentum. The reader who wants to delve more deeply into the details is referred to standard text books in solid-state physics.[43]

In order to give a more chemical meaning to the k value, let us now consider the wave function (3) at two specific k points, $k = 0$ and $k = \pi/a$. From (3) we obtain

$$k = \frac{\pi}{a}\colon\ \psi_{\pi/a} = \sum_{r=0}^{N-1} e^{i\pi r}\phi_r = \sum_{r=0}^{N-1} (-1)^r\phi_r \tag{6}$$

$$k = 0\colon\ \psi_0 = \sum_{r=0}^{N-1} \phi_r$$

These wave functions are depicted in 5. We can see that

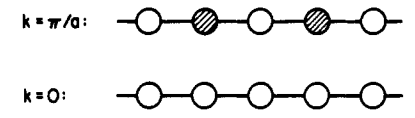

5

ψ_0 is the most bonding wave function, one with no nodes. $\psi_{\pi/a}$, on the other hand, is the most antibonding wave function possible, with the maximum number of nodes. In the range between $k = 0$ and $k = \pi/a$ the nodal structure of a wave function is not observed so easily, due to the complex coefficients in eq 3. Here another important feature comes into play. It is obvious that the energy of a certain k state does not depend on the sign of the k value. Thus, the energy values are 2-fold degenerate for each k value ($E(k) = E(-k)$), except for $k = 0$ and $k = \pi/a$. This degeneracy allows us to form linear combinations of ψ_k and ψ_{-k} with real instead of complex coefficients for the ϕ_r. The reader may verify for himself that the number of nodes increases with k for these real wave functions. Hence, k serves as a node counter.

Physicists have an efficient way of drawing the energy levels of periodic structures. They do not just stack the levels above each other, as in a usual MO diagram (Figure 1a), but draw them as a function of k, as shown schematically in Figure 1b for the linear H chain. For a very large number N of unit cells, the N discrete k values in the first Brillouin zone become very dense and the energy levels represented by points in an $E(k)$ diagram are pictorially indistinguishable from a continuous curve. This curve is called an energy band. Usually, the band is drawn only for positive k values, because, as already mentioned, $E(k) = E(-k)$. The qualitative shape of the hydrogen 1s band is obvious. Since the number of nodes and, thus, the

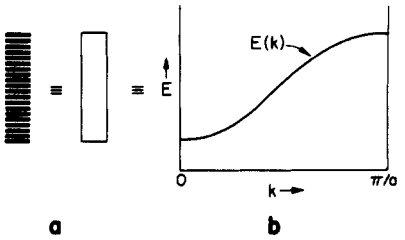

Figure 1. Representations of energy levels for periodic structures in the form of an MO diagram (a) and in an energy vs k (band) diagram (b).

number of antibonding interactions, increases with k, $E(k)$ also increases with k, i.e., the band "runs up". In a Hückel model there is actually a simple closed expression for the energy, $E(k) = \alpha + 2\beta \cos ka$. α and β are the Coulomb and resonance integrals, respectively.

Two notes of caution are appropriate at this point. First, it is not always the case that the number of nodes increases with k. This is true for s orbitals, but imagine a linear array of p orbitals oriented along the chain axis (6). In

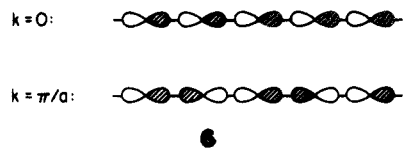

that case the number of nodes has its maximum at $k = 0$ and its minimum at $k = \pi/a$. Thus, the p band "runs down" instead of "up" (the reference is the "zone center", $k = 0$). This means that the energy of the $k = 0$ level is higher than that of the $k = \pi/a$ one. Second, the symmetry-adapted Bloch sums are not automatically eigenfunctions of the Hamiltonian. For the linear H chain, in analogy to the H_2 molecule, the wave function is completely determined by symmetry. For more complicated structures with several orbitals in one unit cell, however, we have to set up Bloch sums for each of these orbitals. In general, only linear combinations of these Bloch sums, not the individual Bloch sums themselves, are eigenfunctions of the Hamiltonian.

One important feature of a band is its band width or dispersion. Let us again consider the linear hydrogen chain. If the distance between neighboring atoms were large we would not expect much interaction, just an ensemble of noninteracting H atoms, each with an electronic energy of −13.6 eV. Thus, in our band structure plot, each of the N energy levels would have an energy of −13.6 eV, resulting in a completely flat band. As the H atoms get closer they start to interact, due to an increasing overlap of their 1s orbitals. This results in a greater splitting of energy levels at different k values, in analogy to the splitting of the two energy levels of the H_2 molecule. The process can be seen in Figure 2, where we have shown the extended Hückel band structure of the H chain for different H–H distances. Note the greater band width as the chain spacing decreases. In the case at hand, the asymmetry of the bands (that the top half of the band is more spread out in energy than the bottom half) is a consequence of including overlap in the calculations.

Throughout this paper we will illustrate actual computations by the extended Hückel method.[35] This is an approximate MO methodology, which has deficiencies but also the advantage of being transparent. Band structures generated by other, often better methods, are not that different,[15,32] since much of what we will focus on is largely determined by symmetry.

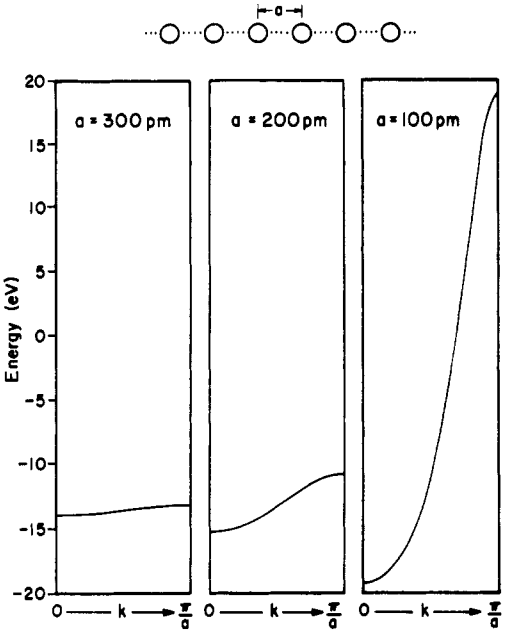

Figure 2. Band structure of a chain of hydrogen atoms spaced 300, 200, and 100 pm apart. The energy of an isolated H atom is −13.6 eV.

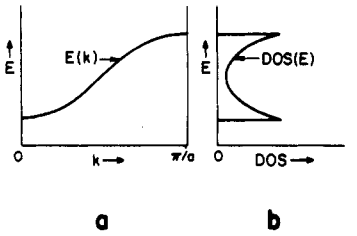

Figure 3. Relationship between a band (a) and a density of states (DOS, b) representation of energy levels.

How many levels of a band are occupied? In our example of a chain of N H atoms we have N energy levels, each of which can be occupied by two electrons of opposite spin. Since the neutral system consists of N electrons, the $N/2$ lowest levels are occupied in the ground state of a "low-spin" system. Thus, the band is half-filled. The energy of the highest occupied level (the HOMO) is called the Fermi energy.[44] In general, the band occupation depends on the electron number.

For a chemical interpretation of the band structure we need two further important tools. One is the density of states (DOS). The number of states in an infinitesimal interval dE between E and $E + dE$ on the energy scale is given by $DOS(E)\, dE$. The DOS for the H chain is shown in Figure 3b. Since the k values are equally spaced along the k axis, the density of states is high in the flat regions of the band. In general, the DOS is proportional to the inverse of the slope, dE/dk, of the band. Comparing Figure 3a and b, it seems as if we get no new information from the DOS. This is true for the simple hydrogen chain. In more complex systems, however, the band structure can get complicated, with many bands overlapping and crossing each other. Here the DOS allows us to spot immediately the location of bunches of energy levels on the energy scale. Most importantly, the DOS can be broken down into individual atomic orbital or atom contributions or even fragment molecular orbitals, showing us how such levels are shifted in the composite structure. The DOS curves of component atoms and atomic or fragment orbitals are called projected DOSs or local DOSs, contributions to the DOS.

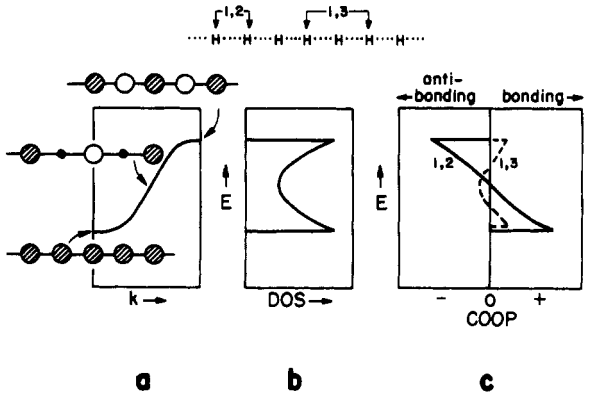

Figure 4. Schematic band structure (a), density of states (b), and crystal orbital overlap population (c) for a chain of hydrogen atoms. In (a) we have indicated the orbital pattern for $k = 0$, $\pi/2a$ and π/a. The COOP in (c) is shown for both first and second nearest neighbor H atoms.

Integration of these DOS curves up to the Fermi level results in an occupation number for the orbital in question or in a charge of an atom. One does have to specify a way of partitioning electrons; the Mulliken population analysis is one commonly used scheme.[45] DOS curves can be interpreted in much the same way as MO interaction diagrams. We will see examples of this in the following sections.

The second tool we need is designed to discriminate the bonding features of the energy bands. How can we retrieve local bonding characteristics in the band structure? To illustrate the problem we consider a two-center molecular orbital:

$$\psi = c_1\phi_1 + c_2\phi_2 \tag{7}$$

The normalization condition for this orbital results in

$$\int |\psi|^2 \, d\tau = 1 = c_1^2 + c_2^2 + 2c_1c_2S_{12} \tag{8}$$

with the overlap integral

$$S_{12} = \int \phi_1\phi_2 \, d\tau \tag{9}$$

The third term on the right side of eq 8 is called the overlap population,[45] because it indicates the electron density in the bonding region between the two centers. This contribution ($2c_1c_2S_{12}$) may be bonding (positive) or antibonding (negative). In general, there are many occupied states, each contributing a term like the third one in (8) to the overlap population between the two atomic orbitals. In most cases one is interested in overlap populations between atoms rather than between specific orbitals. Then it is necessary to sum up the contributions of all possible combinations of atomic orbitals at the two centers. For complex coefficients, as, for example, in Bloch sums, the overlap population term in (8) looks a little bit more complicated but its basic features are the same.

In the case of a periodic structure one considers an energy interval dE at an energy E and weighs the DOS(E) with the average contribution of the levels in that interval to the desired overlap population. The result is an overlap-population-weighted density of states, which is called COOP (crystal orbital overlap population). Integration of a COOP curve up to the Fermi level results in a total overlap population, which indicates the bond strength.

The COOP curves for nearest and second nearest neighbors in the H chain are shown in Figure 4c. As could be expected from our discussion of the nodal properties (see 5), the states at the bottom of the band (near $k = 0$) are the most bonding ones, whereas the states at the top (near $k = \pi/a$) are most antibonding for nearest neighbors. For second nearest neighbors, however, we have a bonding situation both at the bottom and at the top of the band, as can be seen from the wave functions (5 or Figure 4a). Maximum antibonding for the 1–3 interaction occurs at $k = \pi/2a$, as indicated by the corresponding wave function shown in Figure 4a. The amplitude of the second nearest neighbor COOP curves is smaller than that of the nearest neighbor one because $S_{12} > S_{13}$.

C_n Chains

It is time to begin. The starting point for our construction is a linear carbon chain (7). If we take a single

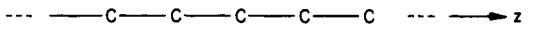

7

carbon atom as the repeat unit or unit cell, we can easily draw the most bonding and most antibonding combinations of the carbon's one s and three p orbitals—much like drawing bonding and antibonding molecular orbitals. These special crystal orbitals for a linear carbon chain are shown in 8 and 9.

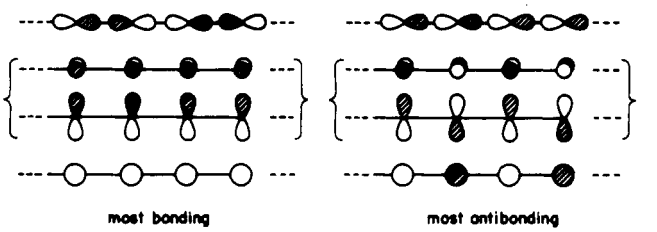

8 9

The orbital combinations for p_x and p_y (hereafter abbreviated as x and y, respectively), the p orbitals perpendicular to the chain propagation axis, are of course of the same energy (or degenerate). We see from 8 that s, x, and y give the most bonding crystal orbital when the unit cell (here a single carbon atom) orbitals are all in-phase, i.e., have the same sign. This is the $k = 0$ (termed Γ) Bloch function. Conversely, the most antibonding crystal orbital, 9, has the unit cell orbitals all out-of-phase, or, in other words, each second unit cell has a different sign. This is the wave function at the Brillouin zone edge, traditionally called Z. For the p_z (hereafter z) orbitals on the other hand, the reverse is true in both cases: Its out-of-phase combination in 8 ($k = \pi/a$, Z) is most bonding while the in-phase one in 9 ($k = 0$, Γ) is most antibonding.

We can now construct the band structure for a linear carbon chain. The s and the degenerate x/y band run up from the all-in-phase combination at $k = 0$ to the all-out-of-phase combination at $k = \pi/a$. The z band, of course, shows the opposite behavior—running down from $k = 0$ to $k = \pi/a$. This is indicated in Figure 5. The C–C distance here is an unrealistic 220 pm. We ask the reader to bear with us for spending some time in discussing this polymer first rather than one with a more realistic C–C separation of 140–150 pm. The reason for studying the longer C–C separation first is that it yields orbitals easy to understand. Those of the more realistic chain are characterized by complicated, but as we will see understandable, mixing.

The energy difference between the highest (most antibonding) and lowest (most bonding) level in a band is called the band width or dispersion. As for the bonding/antibonding splitting in molecular systems, the band width

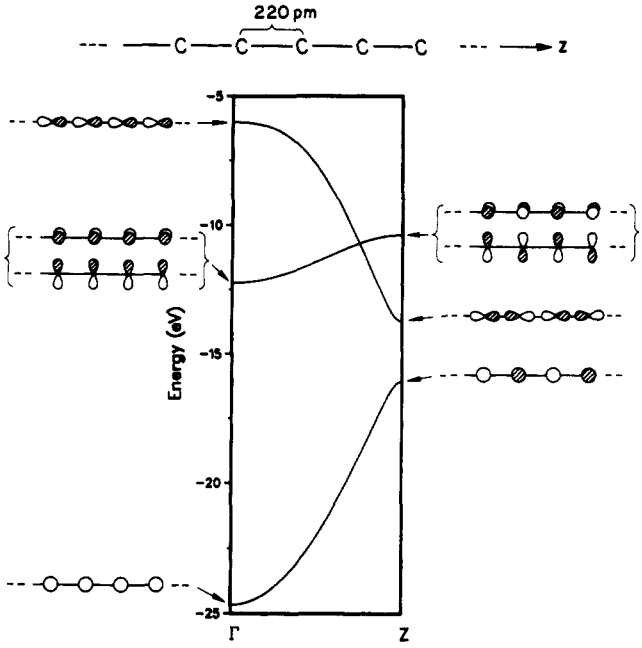

Figure 5. Band structure diagram for a linear carbon chain with C–C of 220 pm and one carbon atom per unit cell. The crystal orbitals are sketched schematically at Γ and Z.

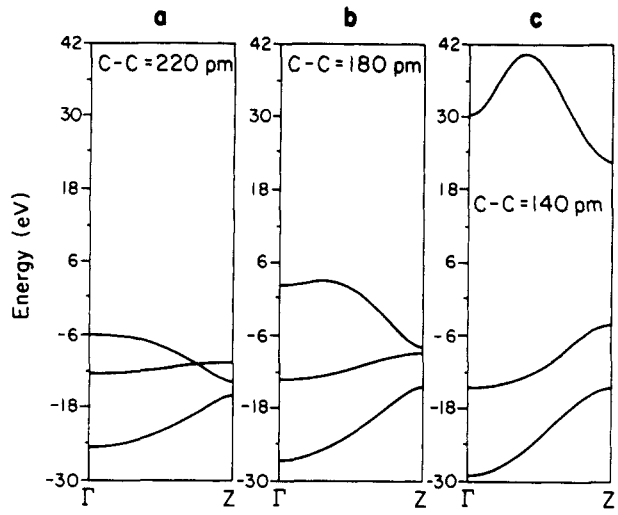

Figure 6. Effect of the inter-unit-cell distance on the band dispersion. Band structure diagrams for linear, bare carbon chains with C–C of 220 (a), 180 (b), and 140 pm (c).

is determined by the interaction (overlap) between orbitals on neighboring atoms (actually unit cells), which in turn depends on the type of orbitals involved and the inter-unit-cell distance. Other things being equal, σ bands (just like bonds) generally have a larger dispersion than π, and these in turn are wider than δ bands. Figure 5 clearly shows that the degenerate π band has a smaller width than the two σ (s and z) bands.

What happens when the C–C distance in the chain goes from the unrealistically long 220-pm to a 140–154-pm separation, appropriate to a polyacetylene or polyethylene? Figure 6 shows three stages of the bond contraction, from 220 to 180 to 140 pm. Note the increase in band dispersion.

But something more than band broadening happens. There is an obvious change in the shape of the bands, and when we examine the DOS and COOP plots in detail we see many changes. Yet what seems complicated is really a relatively simple consequence of two phenomena familiar to molecular theory: s–p mixing and avoided crossings. We will examine them in Figure 7, which compares the band structures, DOS, and COOP curves at C–C of 140 and 220 pm.

Orbital Mixing. At large C–C separation the s and z bands are not much dispersed. They are of almost pure s and p character. You can see this clearly in the DOS curve at C–C of 220 pm in Figure 7a. The analogous DOS curve in the same figure at 140-pm separation is quite different. Now the broad lower band has substantial z character. This is a typical orbital mixing phenomenon; lower lying states of a certain orbital type (s in our case) often manage to enhance their bonding or diminish their antibonding character by mixing in higher lying states of a different type (p in our case) but of the same symmetry. The effect operates as much for homonuclear diatomics as for Cu^+ ions clustering.[46] **10** shows the nature of the mixing schematically.

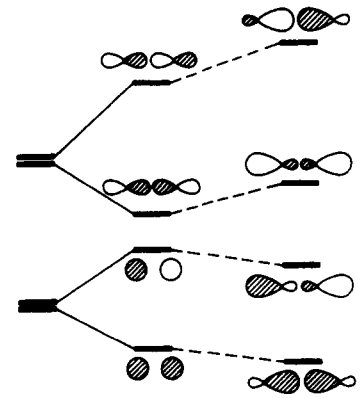

10

Another way to describe what happens is that as one lowers the C–C distance, the resulting bands (mixtures of s + z except at the zone boundaries) evolve from being best described as simply s and z, to a C–C σ and σ^* band description, as depicted in **11**.

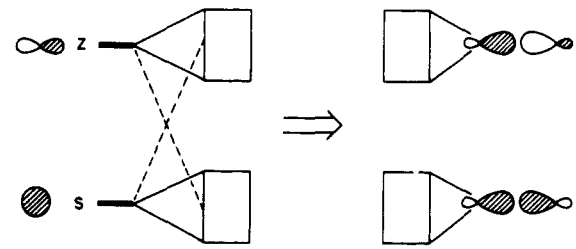

11

In general, s and z Bloch functions are of the same symmetry, although there is no such mixing at the zone boundaries, Γ and Z, where additional mirror planes perpendicular to the z axis (through and in-between the atom centers) render the s and z band symmetry distinct. But in the interior of the Brillouin zone, s and z orbitals can mix. This is a phenomenon of some generality, so let examine it in detail. Consider the half-way point between Γ and Z, $k = \pi/2a$. We have already introduced the orbital pattern at this k point (see Figure 4a). The orbitals of this half-way point for the pure s and z bands and their mixing are illustrated in **12**. The reader will notice that we are drawing two degenerate crystal orbitals for s and z, respectively, and their combinations after interaction. As we mentioned earlier, the MOs of a chain with cyclic boundary conditions come in degenerate pairs. It is this degeneracy that allows us a degree of freedom in the choice of the corresponding orbitals and to form linear combi-

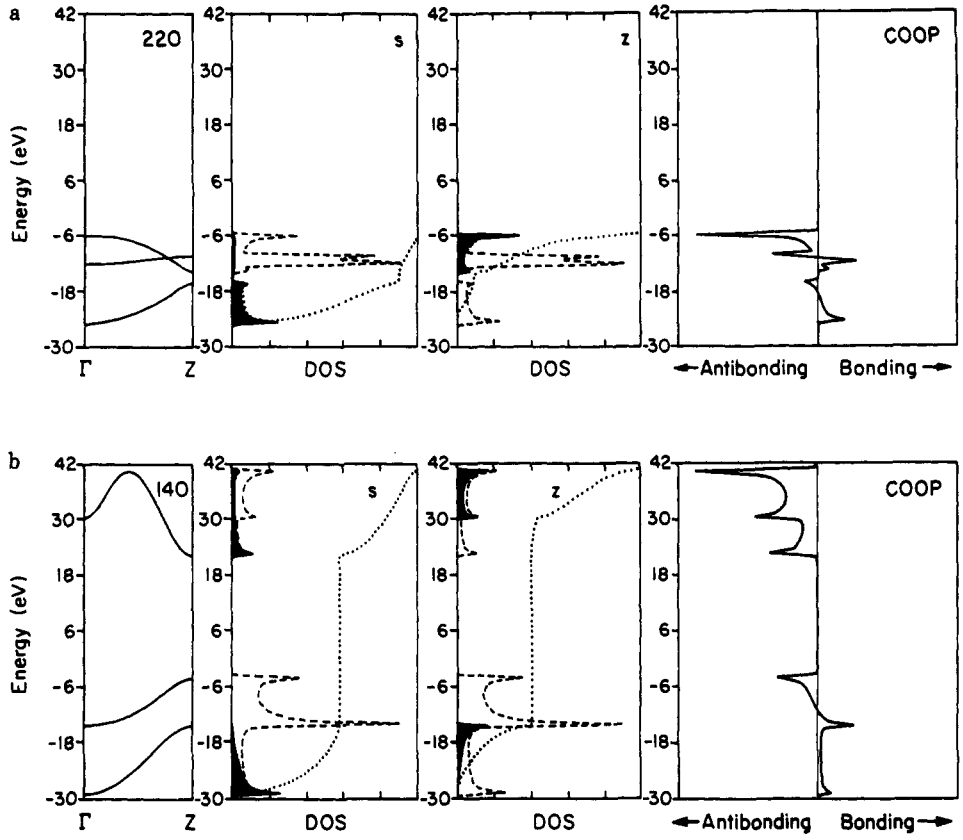

Figure 7. DOS and COOP plots for linear, bare carbon chains with C–C of 220 (a) and 140 pm (b). The s and z orbitals are projected out in the DOS (shaded area) to illustrate the s–z mixing and the character exchange upon an avoided crossing. The total DOS and integration of the respective projected DOS are given as dashed and dotted lines. COOP plots in the right-hand panels demonstrate the bonding/antibonding characteristics of the σ bands and the change associated with the s–z orbital mixing. The band structures are repeated at the left side of the DOS plots to again illustrate the relationship between these bonding characteristics.

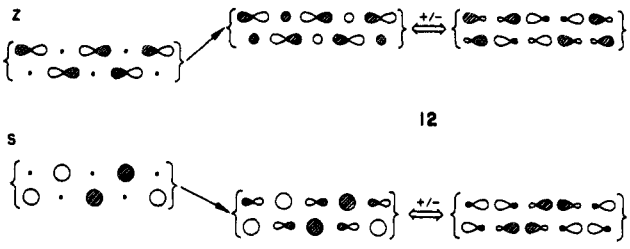

nations of them in order to obtain orbital patterns suitable for a chemical interpretation. This becomes obvious when we sketch the s–z mixed wave functions either with plain s and z orbitals (12 center) or with sp hybrids (12 right). Both representations are interconvertible by taking + and − combinations of the respective two original wave functions.

The s–z mixing is, of course, a function of the C–C distance and affects the shape, orbital, and bonding character of a band substantially. Orbital mixing phenomena are essential to our chemical approach to band structures. They tend to make the interpretation of the diagrams complicated, but at the same time they allow a building of bridges to localized chemical viewpoints.

Avoided Crossings. In molecules two levels of the same symmetry in general are not allowed to cross as a consequence of some geometrical perturbation. In extended structures there is a related noncrossing rule, now relevant to bands that are of the same symmetry and that might cross if interaction between them were not allowed. Once those interactions are turned on, the bands may not cross. However, their wave functions do effectively cross, by which we mean that the bands change character as if their lines had actually crossed.

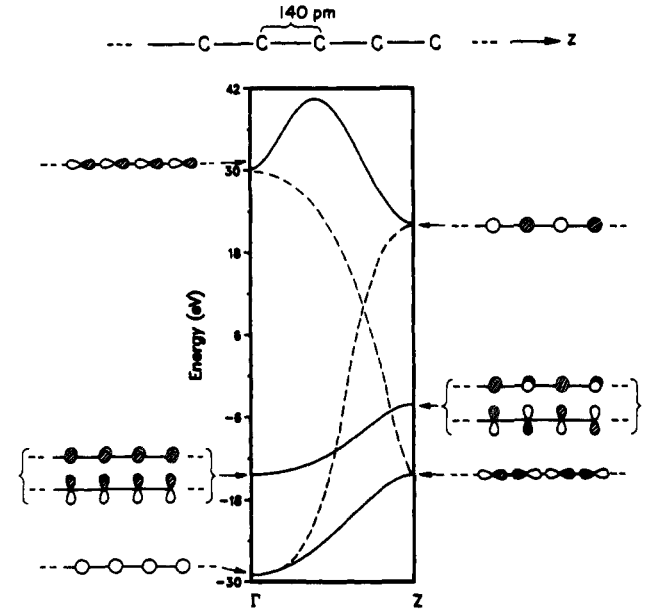

Figure 8. Illustration of an "avoided crossing" in the band structure diagram of a linear, bare carbon chain with C–C of 140 pm. The dashed lines indicate the curves if the bands were allowed to cross, thereby sketching the character exchange for the wave functions. At Γ and Z the crystal orbitals are drawn schematically.

This is best illustrated by an example. At 140 pm both s and z bands are wide. If there were no s–p interaction they would cross (see dashed lines in Figure 8). But the very strong s–p interaction inside the Brillouin zone forbids the crossing, and the bands "repel". The "character exchange" in that avoided crossing is illustrated by the orbital sketches in Figure 8.

Another way to illustrate the avoided crossing derives from a partitioning of various contributions to the DOS. Figure 7 compares the contributions of carbon s and z orbitals to the total DOS, at two C–C separations (dark shaded areas in two middle panels). It is sometimes easier to follow mixing by looking at the integrated occupation of the specified orbital, from $E = -\infty$ on up; plotted on a scale from 0% (left) to 100% (right). That is the dotted line in the two central panels, much like an NMR integration.

Even at the long C–C distance of 220 pm there is a 10% mixing of z into s and vice versa, easiest followed by the integration. The top and bottom of each band are clearly pure s or z in character. Basically this is also true for short C–C separation, Figure 7b, but now the top (at k = Z) of the lower band, which starts out as pure s, becomes pure z (bonding) in character. There has been an avoided crossing. Consequently, the bottom of the upper band (originally pure z) ends with only s (antibonding) character. According to the integration of the projected DOS, the mixing now reaches 40%. As a consequence of this interchange of character from s to z, the lowest band is now C–C bonding throughout (see COOP curves).

Let us at this point give a qualitative description of the electronic structure of this carbon chain. 13 may be a

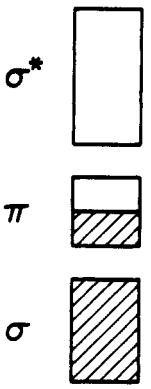

13

useful "block" band summary. At low energies there is a C–C bonding band, at high energy a σ^* band. In between lie two degenerate π bands, which have room for four electrons per carbon. For a neutral C_n chain these bands would be half-filled.

Is linear C_n a hypothetical material? Until recently, one would have said "probably". There is an experimentally unresolved, extensive literature on "karbin" (carbyne),[47] a supposed allotrope of carbon containing just such chains. But recently excellent evidence for the synthesis of carbyne, with polyyne chain lengths of 10–65, by Akagi and co-workers[42] has been presented. One looks forward to the chemistry of this material. What is already certain experimentally[42] and theoretically[48] is that the polymeric material has localized C≡C and C—C bonds, instead of the equal bond lengths we assumed. We will return to this bond localization soon, in the context of polyacetylene.

We built a linear carbon chain from a one carbon atom unit cell. It would, of course, also have been perfectly legitimate to have taken two (or three, four, ...) carbon atoms in the unit cell. In what follows, we will quickly construct the band structure for C_2 as the repeat unit and show its relationship to the one C/unit cell diagram. The reason for doubling the unit cell is that just such an enlargement is necessary in preparation for forming polyacetylene and polyethylene.

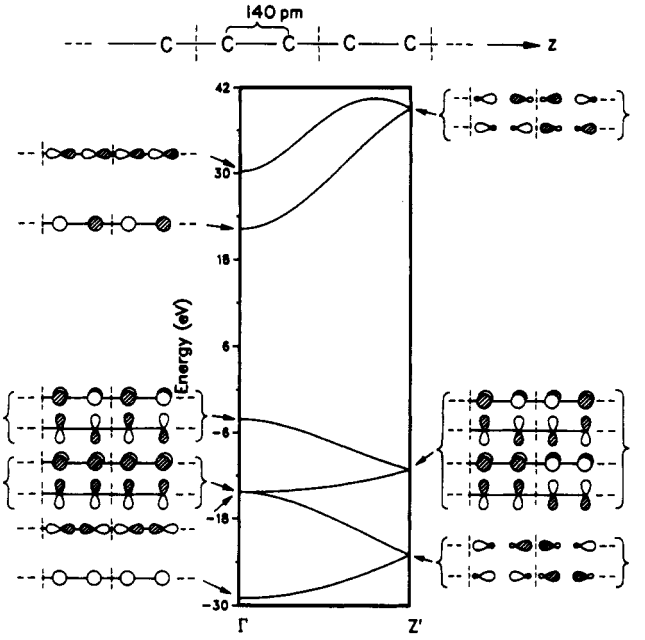

Figure 9. Band structure diagram for a linear, bare carbon chain with C–C of 140 pm and two carbon atoms as a unit cell. The crystal orbitals are given at Γ and Z'.

For the band structures in Figures 5–8, we essentially took the carbon atom orbitals and spread them into bands by going from the all-in-phase to the all-out-of phase combinations. With C_2 as the repeat unit we will do the same, starting from the C_2 molecular orbitals, shown in 14.

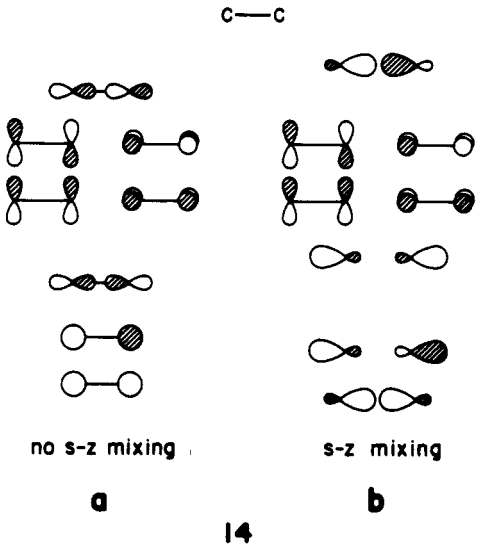

14

Each orbital will give rise to a band. For the all-in-phase combinations at Γ, where s and z are symmetry distinct, no s–z mixing disturbs the picture. We propagate the molecular orbitals in **14a** to give us the appropriate crystal orbital, sketched in Figure 9. At Z' in Figure 9, where s–z mixing is now allowed, the all-out-of phase combinations have to be constructed from the hybrid orbitals in **14b**.

By comparing Figure 9 with Figure 8, the reader may realize that the orbital illustrations in Figure 9 at $k = 0$ are—unit cell boundaries aside—exactly the ones sketched in Figure 8 at $k = 0$ *and* $k = \pi/a$. What we have done (what we have *had* to do) with the band structure of Figure 8 in doubling the unit cell size is just to "fold it back" to give the band structure in Figure 9. This is illustrated

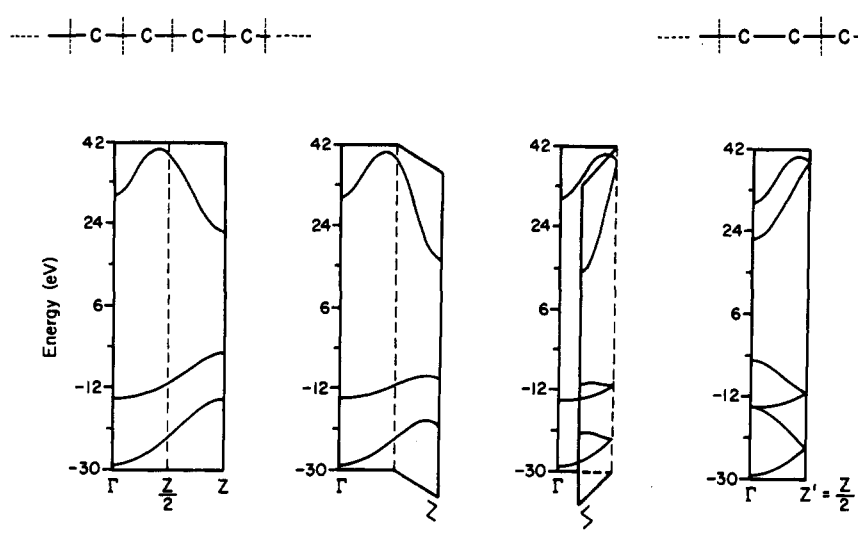

Figure 10. Illustration of the folding relationship in band structure diagrams when doubling (conversely cutting in half) the unit cell size. Here, we go from a unit cell of one C atom to two C atoms in a linear, bare carbon chain (C–C = 140 pm). For crystal orbital representations compare Figure 8 and 9.

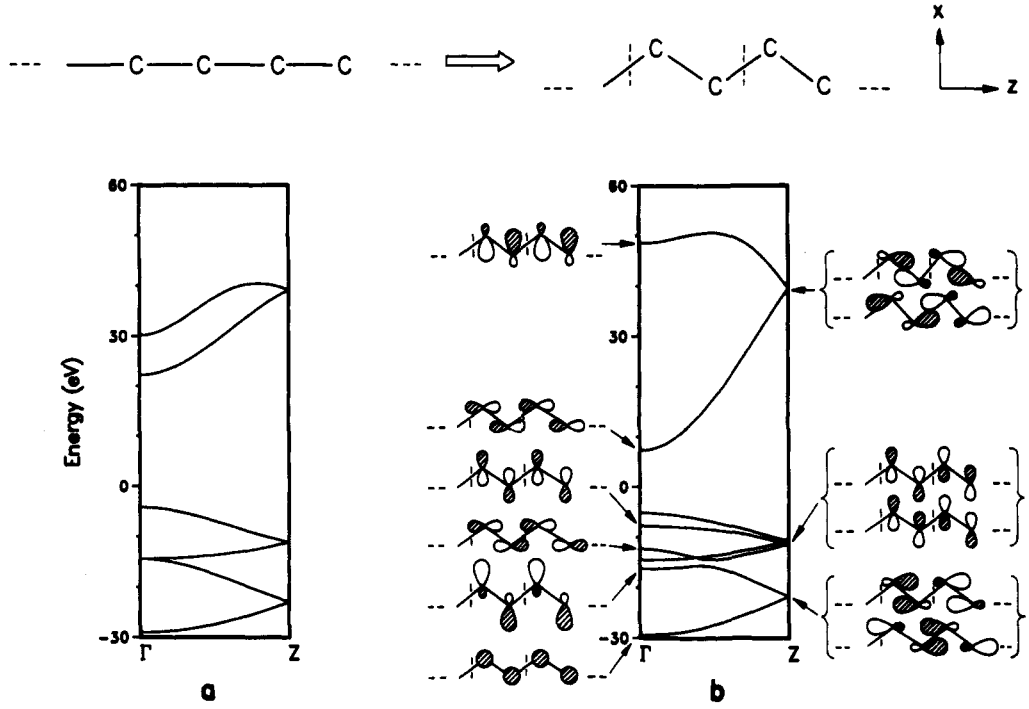

Figure 11. Comparison of the band structure diagrams for a linear (a) and kinked (b) bare carbon chain (C–C 140 pm). Notice the loss of degeneracy of the π band. Crystal orbitals are sketched schematically for (b) at Γ and Z, except for π_y, the π orbitals perpendicular to the plane formed by the carbon backbone. Crystal orbitals for (a) were given in Figure 9.

graphically in Figure 10. It may also help answer the following question which might have arisen in the reader's mind: Why were s and z symmetry distinct at Z in Figure 8, but not anymore at Z′ in Figure 9? The back-folding process clearly demonstrates that Z′ corresponds to the former midpoint between Γ and Z, whose orbital representation we had already sketched in **12** for the s and z, or better σ and σ^* bands. Figure 9 may also help us to understand why we had to draw two degenerate bands in **12**.

A word is in place here about this "folding back". It seems like a theoretical trick, but it is in fact an essential fact of life in describing the electronic structure of polymers. If there is no geometrical distortion, than one can choose one's unit cell in an arbitrary way. Usually one takes the smallest (primitive) cell, but there may be good reasons—chemical sense, ease of analysis, preparation for a subsequent distortion—for choosing a larger cell. The orbitals do not care what cell we use; they are the same orbitals. If we choose a large unit cell, all that we are doing is plotting the very same orbitals—no more, no less of them in number, unaffected in energy—in a different way. Because the orbitals are the same, the DOS and COOP curves describing the two choices are precisely the same.

To prepare for the construction of the polyacetylene and polyethylene band structures we now proceed to introduce a kinking distortion in the carbon chain (**15**). The kinked chain has two carbon atoms as the smallest unit cell. We anticipate that the degeneracy of the π orbitals will be lost and that the π orbital that lies within the plane of the chain will mix with the σ orbitals to give what might be called a lone-pair band. The band structure diagram for the linear and kinked chain (both with C_2 as

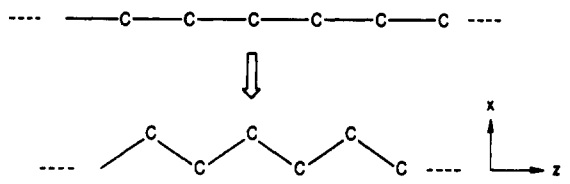

15

the repeat unit) are contrasted in Figure 11. The crystal orbitals for the kinked chain are illustrated at some special points.

What happens when the chain kinks is pretty simple. There is some change in the dispersion of the σ bands, but it is one member of the formerly degenerate π band that is most dramatically affected. It loses its π symmetry and splits off from the remaining π component, the one consisting of y orbitals perpendicular to the kinking plane. The π y band is essentially unaffected. The split-off π x band mixes in s character, as expected. This may be seen in the x and y projections of Figure 12. The mixing is not great; the x band remains mainly such. Note also the new avoided crossing between that in-plane π band, now of σ symmetry, and a σ band.

Polyacetylene

Let us begin with *all-trans*-polyacetylene. At first we assume equal C–C bond lengths, i.e., no bond alternation within the carbon backbone (16). We will compose this polymer from the kinked carbon chain as one fragment and the hydrogens alone as another sublattice. The band structure of the two sublattices and the composite structure is shown in Figure 13. The two hydrogen bands are simple, narrow because of the large H–H distance in the sublattice.

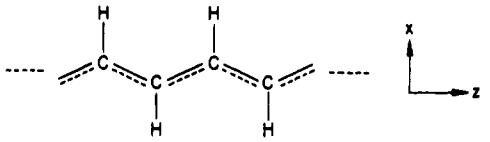

16

The important interaction takes place between the two x bands of carbon (labeled in accordance with the coordinate system shown in 16) and the H bands. This interaction is favored by the good energy match of these bands and by the favorable overlap of the C x and H s orbitals. It is the x orbitals that point to the hydrogens. Remember that the folding-back process described in the previous section leaves us with two bands of each kind, which are joined at Z (two σ_{CC}, two x, two π, and two σ^*_{CC} bands for the kinked C chain). The x band is not of pure C x character, but has s (and in the region of the avoided crossing, z) mixed in. We have chosen this label because of the dominant contribution from the x orbitals and also to indicate its origin in the pure π–x band of the linear C chain.

The interaction of the x bands and the hydrogen bands is nicely recognized in the band structure of the composite polymer. It results in a C–H bonding and a C–H antibonding band, which are shifted down and up, respectively, relative to the x bands. Figure 13 therefore resembles very much a conventional MO interaction diagram.

We have to take care not to be confused by avoided crossings of the bands. The dashed lines in Figure 13 indicate how the bands have to be connected in order to preserve their character. We show the relevant orbitals at Γ for the kinked carbon chain and *all-trans*-polyacetylene in 17. It can be seen that only the x_1 band has some s contribution at Γ whereas the x_2 band is of almost pure p character.

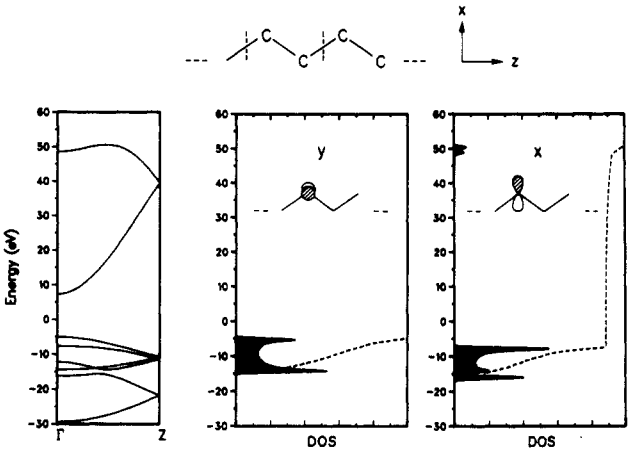

Figure 12. DOS plots for the kinked bare carbon chain (C–C 140 pm) with y and x orbitals projected out to illustrate changes in the x band. The x orbital density around 50 eV is due to the new s–x mixing. The indentation in the projected DOS for x at ~−15 eV is indicative of an avoided crossing between the now σ-symmetrical x band and another σ band (compare to band structure in the left-hand panel). The dashed line is the integration of the projected DOS.

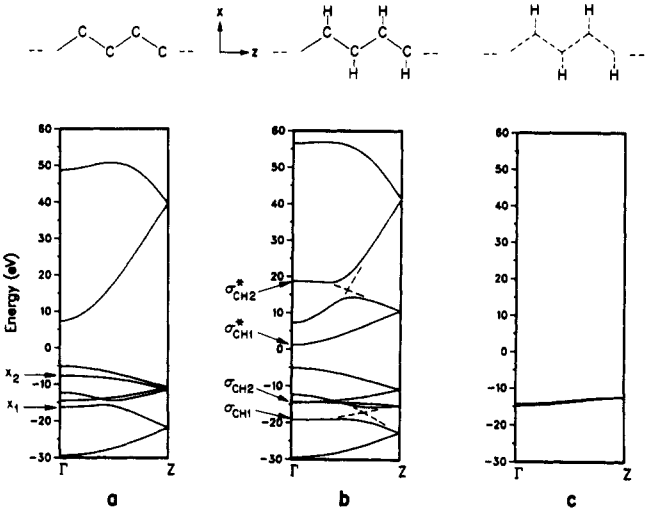

Figure 13. Band structure for the carbon sublattice (a), the hydrogen sublattice (c), and the composite structure (b) of *all-trans*-polyacetylene with no bond alternation (16; C–C 140 pm). Dashed lines should help to visualize avoided crossings. For the band labels at Γ in (a) and (b) see 17.

The mixing just described also shows up nicely in the DOS curves of the hydrogen s and carbon x orbitals, which are shown in Figure 14. Note the coincidence of the peaks for these two orbital contributions. The COOP curve for the C–H bond also present in Figure 14 shows us the bonding and antibonding character of these bands. The "gaps" in the DOS and COOP curves are due to the avoided crossings mentioned above.

It is possible to summarize the gross bonding features of the orbitals of polyacetylene as shown in 18.

We have seen that our gradual approach to polyacetylene leads to an insight into the band structure and facilitates our understanding of it in a natural way. This interpretation would not have been obvious had we just calculated the band structure of the final polymer.

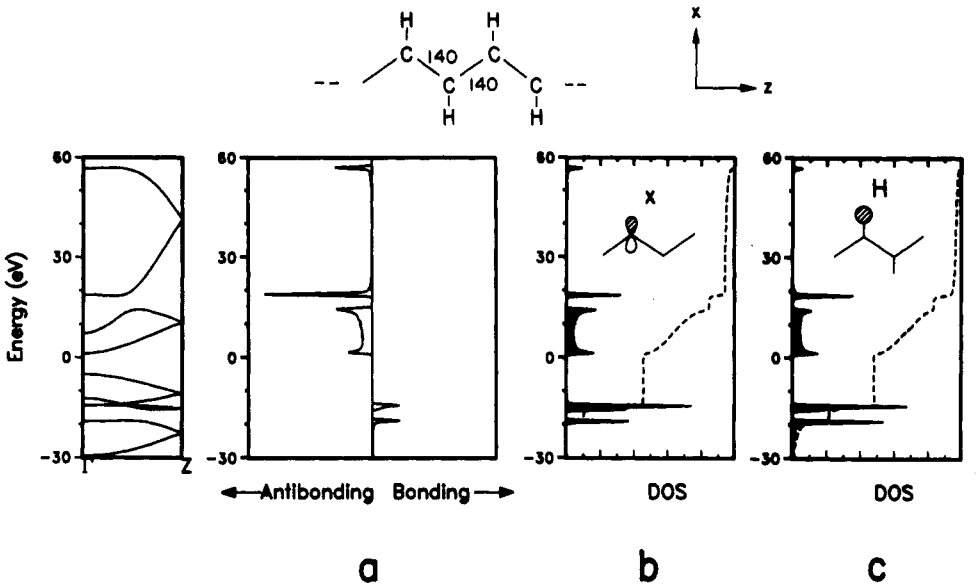

Figure 14. (a) COOP curve for the C–H overlap population in *all-trans*-polyacetylene with no bond alternation (16; C–C 140 pm). The corresponding carbon x and hydrogen s contributions to the DOS (magnified 2.5 times) are shown on the right (b and c) with the integration of the projected DOS given as a dashed line. Note the matching peak positions in (a), (b), and (c).

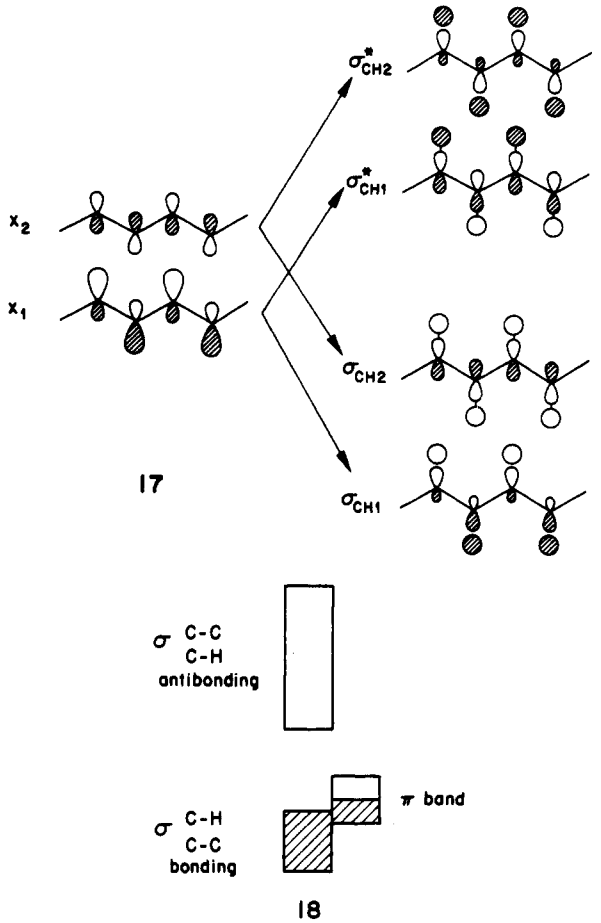

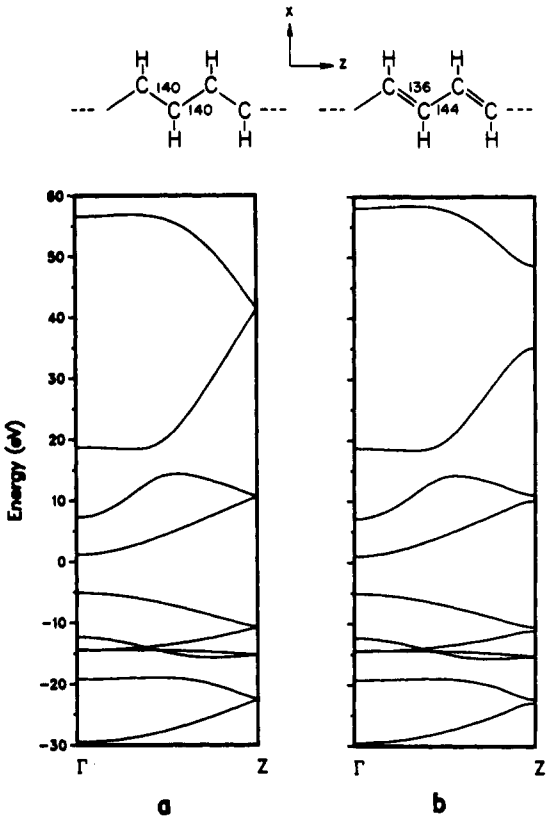

Figure 15. Band structures of *all-trans*-polyacetylene with bond alternation (b; C—C 144 pm, C=C 136 pm) as compared to the one for equal C—C bond lengths (a; C—C 140 pm).

It is known that polyacetylene has unequal C–C bond lengths, alternating long and short. This fact was foreseen theoretically,[49] for reasons that we will discuss below.

Let us introduce that bond alternation within the carbon backbone. So far we have assumed equal C–C bond lengths of 140 pm. The observed values are 144 and 136 pm for the single and double bonds, respectively.[50] The band structure of the bond-localized polymer is shown in Figure 15. We recognize immediately that the degeneracies at Z are removed. These degeneracies had been mandated as a result of the 2-fold screw axis symmetry, which is lost when the C–C bond lengths alternate.

Why is this structure energetically favored? The key is the π band, composed of p orbitals perpendicular to the plane of the polymer. In Figure 15 the effect of bond alternation on the π band is obscured due to the large energy window. Figure 16 reduces the window, showing more clearly the effect on the half-filled π band. The energy levels of that band near the Fermi level at Z are shifted down in comparison with those of the chain with equal C–C bond lengths, whereas the unocccupied π^* levels are shifted up. This results in a stabilization of the bond-localized structure. The other occupied bands do not

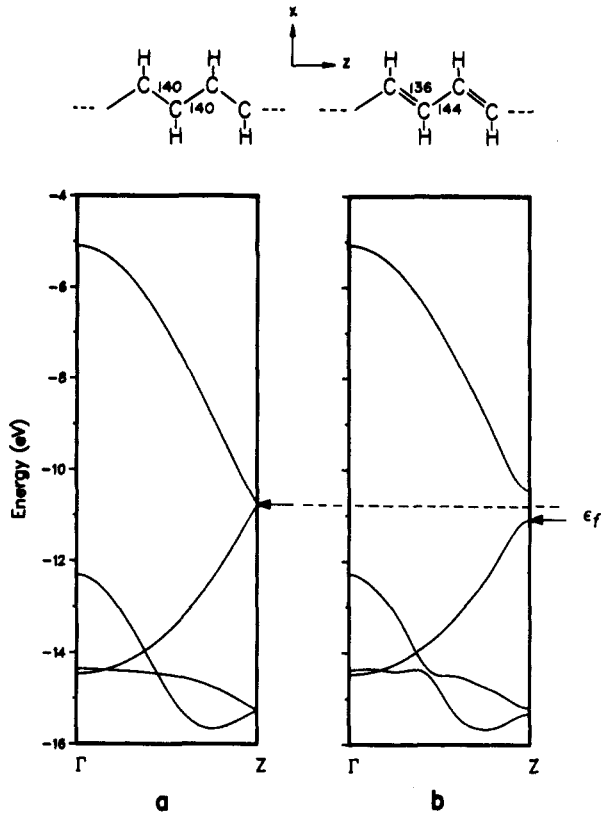

Figure 16. Magnification from Figure 15 of the π band in symmetrical (a) and bond-alternated (b) *all-trans*-polyacetylene to show more clearly the effect of distortion. In (b) the energy levels near the Fermi level at Z are shifted down in comparison to (a), resulting in a stabilization of the bond-alternated structure. Also, note the avoided crossing in (b) between the other two bands included in the panels due to a loss of the 2-fold screw axis symmetry.

change very much in their total energy, because their splitting at Z is approximately symmetrical with respect to the point where the former bands were joined. The bottom part of these bands goes down; the top part goes up in energy. The overall contribution of these bands is slightly destabilizing. The final structure is the result of an energy balance with respect to the two competing effects (stabilization of the π and destabilization of the σ system).

In order to explain the splitting of the π and π^* bands let us take a look at the wave functions of the two bands at Z. The conjugated π system of polyacetylene is quite analogous to the simple H chain. It consists of only one orbital per C atom, a y orbital, which for symmetry reasons cannot interact with carbon orbitals other than y on other carbons. The kinking of the chain only affects second and higher nearest neighbor interactions, which are of minor importance. Remembering the folding back of the bands in polyacetylene, we recognize that the wave functions of the π bands at Z must be analogous to those of the H chain indicated in Figure 4a in the middle of the band. We have redrawn them for polyacetylene in **19** on the left. The boundaries of the unit cell are indicated by the dashed lines.

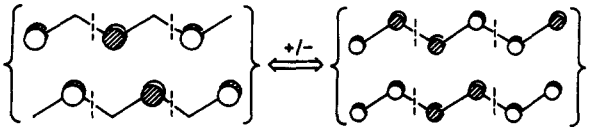

19

Unfortunately, these wave functions are not the proper zero-order wave functions for a perturbation theoretic treatment of the bond length distortion. Since these wave functions are degenerate, however, we are allowed to form equivalent linear combinations. These are shown on the right-hand side of **19**. It is easily recognized that they are obtained by addition and subtraction, respectively, of the wave functions on the left. The wave functions on the right are adapted for the subsequent bond alternation. The degeneracy of these orbitals for polyacetylene with equal C–C spacing is obvious: whereas the lower of the two is bonding within the unit cell and antibonding between cells, the situation is reversed for the upper one, the number of bonding and antibonding first nearest neighbor interactions exactly canceling each other in both cases.

Now we introduce the bond length alternation, as indicated in **20**. We shorten the bond within the unit cell

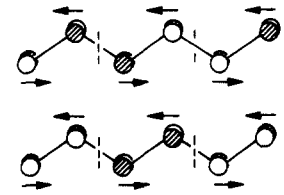

20

and lengthen it between unit cells. Doing it the other way round would not affect our conclusions. For the lower orbital the bonding interaction within the unit cell is strengthened, whereas the antibonding interaction between unit cells is weakened, making this orbital a bonding one and shifting it down in energy. The situation is obviously reversed for the upper orbital, which is therefore antibonding and shifted up in energy. This first-order energy splitting is most effective near Z, where the energy levels of the π and π^* bands are exactly or nearly degenerate. It dies off as we move away from Z (see Figure 16).

The bond length alternation in polyacetylene is an often quoted example of a Peierls distortion, a common phenomenon in one-dimensional systems.[51] The Peierls theorem states that a one-dimensional system with an incompletely filled band distorts in such a way as to open up a gap at the Fermi level. One therefore ends up with a semiconductor, whereas the nondistorted structure would have been a metal. Indeed, the intrinsic conductivity of polyacetylene is low; the spectacular metallic conductive properties emerge only upon doping.

The Peierls theorem is the solid-state analogue of the molecular Jahn–Teller theorem.[52] Perhaps it is worthwhile to review the latter, in the molecular context. Consider, for example, the π system of a square butadiene, **21**.

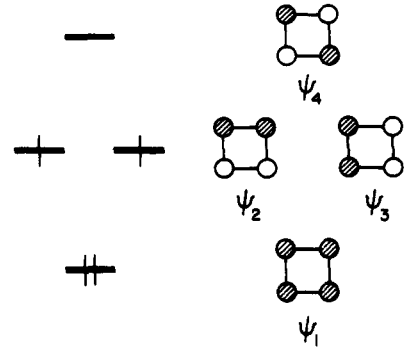

21

We see two electrons in degenerate orbitals. This is the prerequisite for the workings of the Jahn–Teller theorem, which says that in such a situation there exists a stabilizing deformation of the molecule, which destroys that degeneracy. A distortion from a square to a rectangle will do it (**22**).

The orbital workings of this Jahn–Teller distortion are easy to see. By the distortion at the right in **22** or **23**, Ψ_2 is stabilized: the 1–2, 3–4 interactions that were bonding

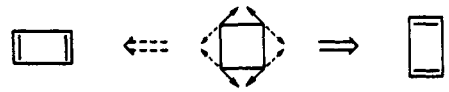

22

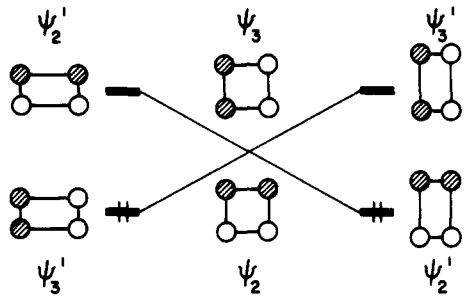

23

in the square are increased; the 1–4, 2–3 interactions that were antibonding are decreased by the deformation. The reverse is true for Ψ_3—it is destabilized by the distortion at the right. If we follow the opposite phase of the vibration, to the left in **22** or **23**, Ψ_3 is stabilized, Ψ_2 destabilized.

Something very similar to this happens in the pairing distortion in the polyacetylene chain. The degeneracy of two orbitals formerly equal in energy is broken by a symmetry-lowering vibration.

Another interesting phenomenon in polyacetylene is the occurrence of bond alternation defects, which are often called solitons. The existence of these bond alternation defects in sufficiently long polyene chains had already been suggested some time ago by Pople and Walmsley.[53] More recently, the seminal work of Su, Schrieffer, and Heeger[7] has stimulated an immense volume of theoretical work on this problem. Its relationship to the mechanism of conduction in doped polyacetylene remains, in our opinion, not settled.[54] Still it is important to see how solitons come about.

A simple valence bond representation of a neutral, a positively charged, and a negatively charged soliton is

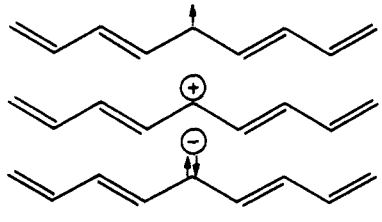

24

shown in **24**. (In the organic chemist's language, one can think of these solitons as radical, carbocation, and carbanion sites, respectively.) The neutral soliton (carbon radical) has no charge but has spin ($s = {}^1/_2, q = 0$), whereas the charged solitons (carbocation or carbanion) are spin-

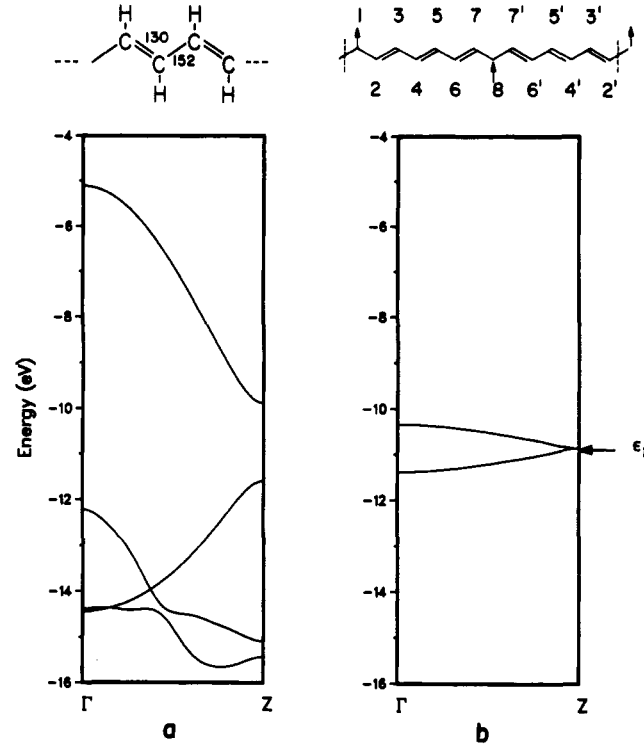

Figure 17. (a) π-band structure of undisturbed polyacetylene with a large bond alternation (C—C 152 pm, C=C 130 pm; cf. to Figure 16b). (b) Soliton–antisoliton band of the disturbed polyacetylene **26** (same bond alternation as in (a); other polyacetylene bands are omitted and hydrogens not drawn for clarity).

less ($s = 0, q = \pm e$). It can be seen that the soliton (represented as a localized radical electron in the neutral case) separates two different bond-localized phases in the chain structure, which differ by the arrangement of their single-bond/double-bond sequence. **24** suggests misleadingly that the original bond alternation pattern, with its difference in single-bond/double-bond lengths of ~8 pm, is restored in the immediate vicinity of the soliton. Actually, the bond length difference is nearly zero near the soliton center and increases only gradually with distance from this center. Correspondingly, the probability density of the soliton wave function is not constrained to just one carbon atom as in **24**, but is smeared out over a certain range of carbon atoms (but not over the whole chain, for it is still pretty much localized). Such an electron delocalization and subsequent adjustment of bond length differences in conjugated systems is also quite familar to chemists.

The soliton is a localized, nonbonding state with its energetic location in the middle of the Peierls gap between the π and π^* bands (**25**). This nonbonding behavior is

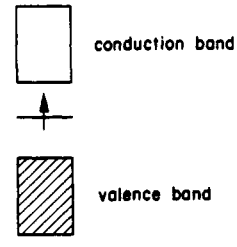

25

reflected in its wave function: even in regions of high probability density there is a chance of finding the electron only on every second carbon atom, being zero at the carbon

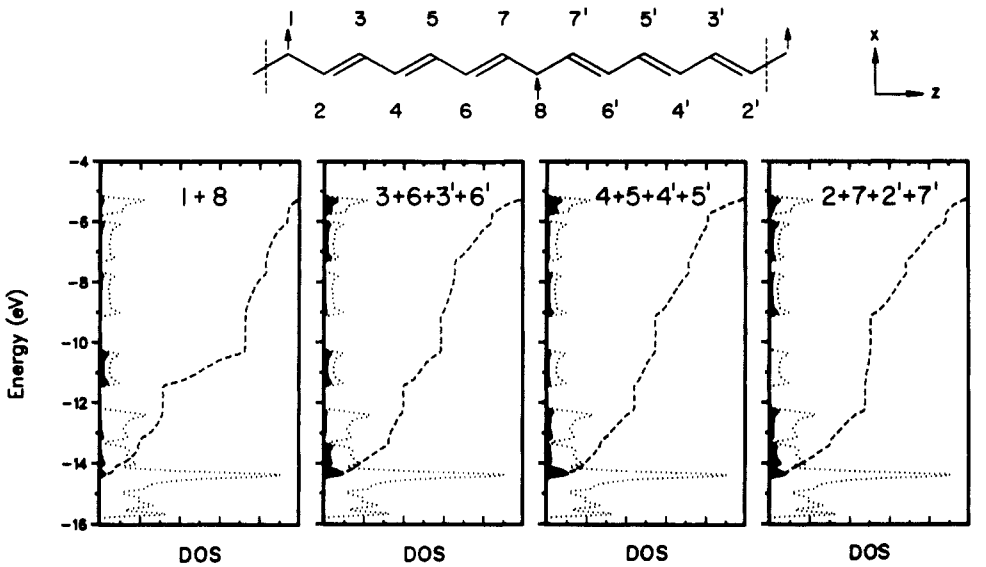

Figure 18. Projected DOS of the π_y orbitals on the different carbon centers in **26** (large bond alternation, C—C 152 pm, C=C 130 pm; cf. to Figure 17). The main contribution to the energy interval from −10.5 to −11.5 eV (midgap states) comes from the soliton–antisoliton centers 1 and 8 in **26**, thus confirming the assignment of the band in Figure 17b. The dotted lines give the total DOS, the dashed lines the integration of the respective projected DOS.

Table I
Charge Densities of the Soliton States at Different Carbon Atom Positions

position	charge	position	charge
1 = 8	0.46	5 = 5′ = 4 = 4′	0.08
3 = 3′ = 6 = 6′	0.21	7 = 7′ = 2 = 2′	0.03

atoms in between.[55] In **24**, the allowed positions of the soliton are the carbon atoms in the upper half of the chain—as a chemist would expect—giving a wave function pattern of alternating positive and zero (in our simplified approach) spin densities.

Is it possible to retrieve some of the soliton properties within our simple tight-binding model? Of course, we cannot treat a single soliton on a long polyacetylene chain, because it destroys the periodicity of the lattice. But how about a regular periodic array of solitons? In order to do this we have to create soliton–antisoliton pairs. This is shown in **26**, where we present one unit cell of a periodic

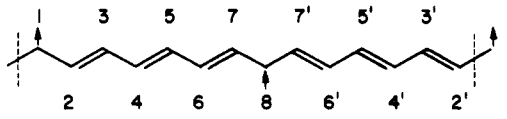

26

array of soliton–antisoliton pairs. The allowed positions of the soliton are the odd-numbered C atoms, whereas those of the antisoliton are the even-numbered C atoms.

The problem with this approach is that the separation distance between the soliton and antisoliton is not large enough to prevent them from interacting with each other. It is therefore desirable to localize the wave function as much as possible. Thus, it is helpful to greatly exaggerate the bond length difference, because this enhances the localization. This was done by assuming bond lengths of 152 and 130 pm for the single and double bonds, respectively (remember the real values in polyacetylene are 144 and 136 pm, respectively). As a compromise between a reasonably large soliton–antisoliton distance and a not too big number of atoms within one unit cell we separate the soliton and antisoliton centers by three double bonds.

The results of the calculation are given in Figures 17 and 18 and Table I. Figure 17 shows the band structure for an undisturbed polyacetylene chain with the large bond alternation mentioned above (130 and 152 pm) (a) and a part of the band structure for the soliton–antisoliton geometry shown in **26** (b). Due to the extensive folding back we show only the soliton bands in Figure 17b and omit the rest of the band structure. We recognize that these bands fit quite nicely into the gap of the band structure in Figure 17a and therefore represent midgap states.

Is there any further indication that the bands in Figure 17b relate to the solitons and antisolitons indicated in **26**? The answer can be found in Figure 18, which shows the contributions of the y orbitals on different C atoms to the total density of states. We recognize that the main contribution to the midgap bands comes from soliton and antisoliton centers 1 and 8, respectively, which are equivalent for symmetry reasons. Moving away from the center of the soliton to positions 3, 5, 7, or, equivalently, 6, 4, 2, the contributions to the midgap bands die off, as could be expected from our description of the properties of the soliton wave function given above. In Figure 18 we have added up the contributions of symmetry-equivalent positions. Thus, all symmetry-equivalent contributions include four y orbitals, except for center 1, which has only position 8 as its equivalent. Some caution is therefore necessary in the interpretation of Figure 18. If we want to compare the contributions of, e.g., positions 1 and 3 to the total DOS in Figure 18, we have to weight the projected DOS in the two left-hand panels of Figure 18 by $^1/_2$ and $^1/_4$, respectively. Please note that the soliton centers 1 and 8 give only minor contributions to the other π bands. The contribution of the soliton bands to the π electron densities at different carbon positions (given in Table I) further supports our picture.

Two final comments on polyacetylene. First, since the infinite polymer is just the extrapolation of a polyene, one should be able to see a relationship between the π levels of ethylene, butadiene, hexatriene etc. and the polymer. Figure 19 shows this quite explicitly; the finite levels of the monomers "build up" quickly to the band structure of the polymer. Second, our discussion here has not done justice to many fascinating aspects of polyacetylene physics and chemistry—the role of electron correlation and its balance with electron delocalization as described by the

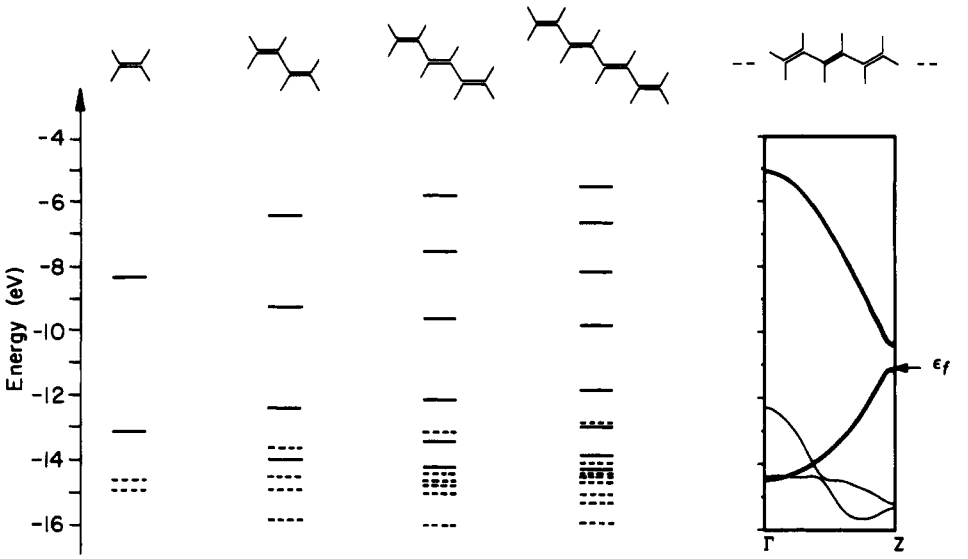

Figure 19. Relationship between the levels of ethylene, butadiene, hexatriene, octatetraene, and polyacetylene around the Fermi energy, illustrating the "buildup" of the polymer band structure. Bold lines represent π orbitals; dashed lines stand for σ levels (cf. Figure 3 in ref 16b).

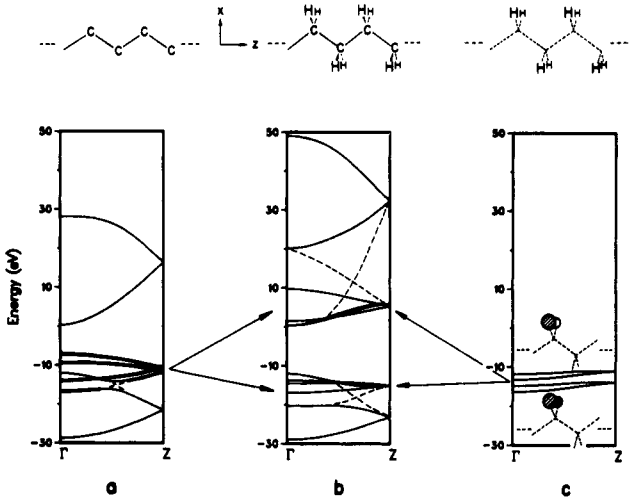

Figure 20. Band structure diagram for polyethylene (b), contrasted to the band structure of its bare carbon backbone (a) and hydrogen fragment (c) (C—C 154 pm, all angles tetrahedral). The carbon x and y bands in (a) are drawn bold; their shift upon interaction with the hydrogen sublattice in (c) is indicated by the arrows to (b). Dashed lines in (b) should visualize the avoided crossings. The hydrogen bands in (c) have been assigned as a symmetric and an antisymmetric combination, with respect to the plane of the carbon backbone.

Hubbard model, and interchain coupling.[5,10,13] The system has been immensely instructive.

Polyethylene

We must construct and analyze the polyethylene band structure in a way that is quite similar to polyacetylene. Shown in Figure 20 are again the diagram for a bare, kinked carbon chain (now C–C 154 pm, C–C–C 109.5°, prepared for a reasonable polyethylene geometry[56]) and the band structure of the hydrogen fragment part of polyethylene. It is no surprise that the hydrogen bands are rather flat, given the long H···H contacts.

We expect the hydrogens to interact mostly with the π_y and the carbon "lone-pair" (x) band of the naked chain—both are highlighted in their fragment band structure. How these bands shift from the carbon fragment to the full band structure diagram of polyethylene is indicated as well. A magnification of the central part of the polyethylene band structure (given in Figure 21) shows more clearly the avoided crossings and the assignment of the C–H bonding and antibonding bands. It is obvious that there are four bonding and four antibonding C–H bands, consisting each of two symmetric, C x, and two antisymmetric, C y, components, respectively, and a hydrogen combination of the same symmetry (the symmetry assignment being made with respect to the plane of the carbon backbone). Because of their different symmetry these C–H bands do not mix and are allowed to cross each other. While the carbon y-H bands are symmetry distinct from all the others, thus not obscured by any avoided crossings or mixings, the carbon x-H bands are of the same symmetry as the C–C σ and σ^* band, therefore giving some mixings and avoided crossings.

Looking at this interaction from another angle, we may form an "MO" interaction diagram, comparing the DOS plots of orbitals for the carbon and hydrogen fragment with those of the full polyethylene chain. Figure 22 traces the hydrogen, carbon s, x, y, and z contributions to the bands. It is useful to decompose the total DOS for the hydrogen fragment (Figure 22c) and the hydrogen orbitals in polyethylene (Figure 22b) into contributions from symmetric and antisymmetric linear combinations and project these out separately. This illustrates more clearly their respective interaction with the symmetric x and antisymmetric y orbital of carbon.

One realizes that the hydrogen interaction with the carbon x and y orbitals is strong. First, these fragment orbitals (Figure 22a and c) have their charge densities concentrated in the same energy interval, from about −8 to −17 eV. The difference in energy between them is small, which is one prerequisite for good orbital interaction. The matching of hydrogen and carbon x/y DOS in the resulting polyethylene crystal orbitals (Figure 22b) illustrates their strong mixing. As a consequence of this interaction most of the x and y band gets pushed up in energy—as indicated by a small marker, at the right in each diagram, specifying the median (50% filling) energy of the given orbital.

A strongly antibonding carbon s- (symmetric) H interaction pushes the (unfilled) top of the s band from ~28 eV to over 50 eV. Changes in the z band—whose median remains unaffected—mainly concern the high-energy part of the band from ~7 to 28 eV. Its disappearance is in

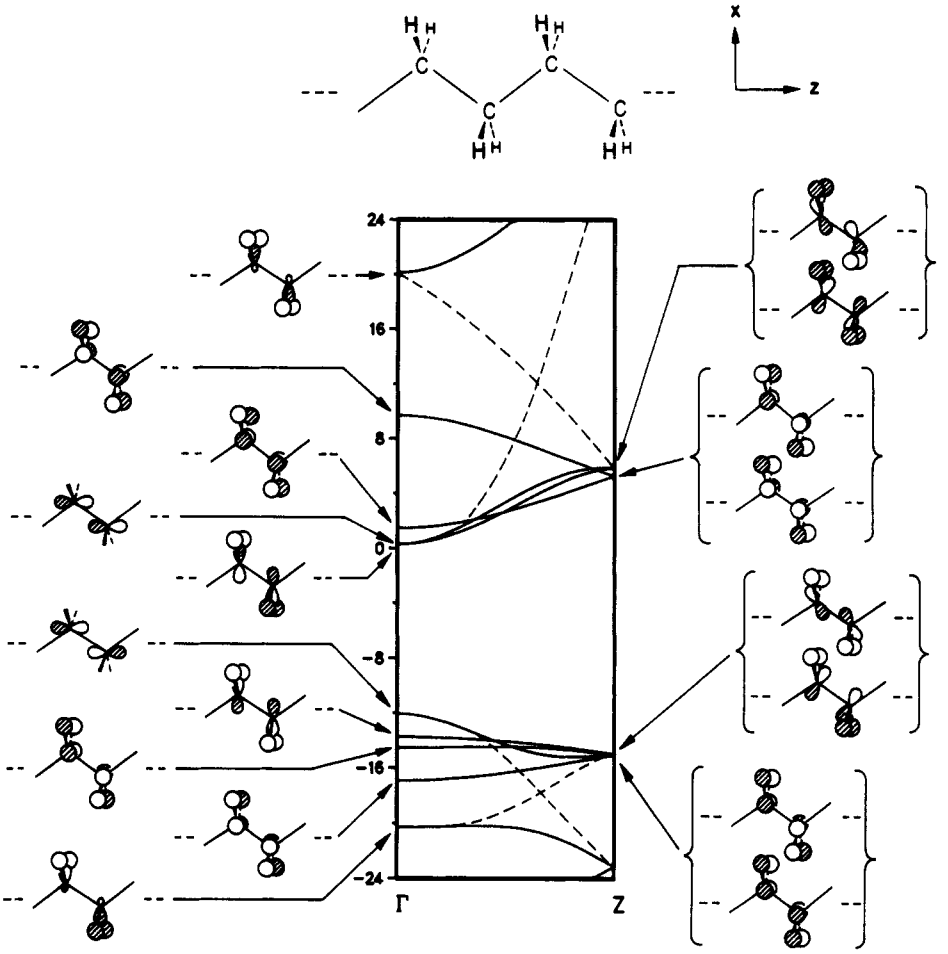

Figure 21. Magnification of the central part of the polyethylene band structure from Figure 20b with orbital sketches for the x-H and y-H bands at Γ and Z. Only the unit cell orbitals are shown, which have to be propagated in-phase at Γ and out-of-phase at Z, to give the respective crystal orbital at this k point. At Γ, the z bands are assigned as well. Dashed lines show the avoided crossings.

turn due to the upshift of the antibonding s orbitals and the subsequent decrease in s–z mixing, which leads to a more concentrated (antibonding) upper part of the z band.

The two carbons and four hydrogens in the unit cell together have 12 orbitals, which give rise to 12 bands. With 12 electrons also available, six of these bands will be filled—right up to the onset of the large band gap at about −12 eV. This band gap of over 10 eV is in agreement with the excellent insulating properties of polyethylene. Two of the filled bands correspond to mainly C–C bands and four to C–H bands, coinciding with the two C–C bonds and four C–H bonds that one might expect in the unit cell just from chemical intuition. The reason that a degenerate pair is always formed at k = Z is to be found in the existence of a screw axis or glide plane as a translational symmetry element (**27**).[57]

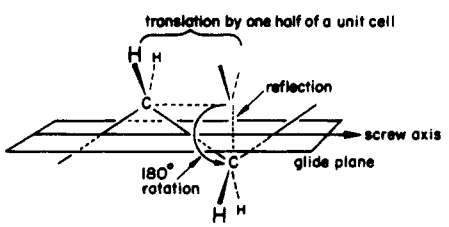

27

The COOP plots in Figure 23 illustrate the C–H and C–C bonding and antibonding character of the polyethylene bands and its carbon fragment. The contrast to the COOP plot for the C–C bands in the carbon backbone fragment illustrates again the obvious shift up in energy of the empty C–C antibonding bands, a consequence of their C–H antibonding interaction. Also, note that only C–C and C–H bands with predominant bonding character are filled. However, some C–H bands do contain some C–C antibonding character, as can be seen from the sketches in Figure 21 and the small blip marked by an arrow at ~−20 eV in Figure 23b. The antibonding C–C contribution in the COOP is mostly obscured by strong C–C bonding contributions from σ_{CC} bands in the same energy region. The appearance of this blip in the polyethylene chain, compared to the carbon-only fragment, is an indication that C–H bonding is more important than C–C bonding.

A comparison of the C–H and C–C overlap population values in polyethylene with those in small molecule models, alkanes, shows only minor departures in ethane and propane from the infinite chain value, while the n-butane values are nearly identical. Figure 24 relates the band structure of polyethylene to the orbital levels in a series of parent alkanes: The molecular orbitals fall nicely within the respective energy ranges spanned by the bands, proving again the close electronic relationship between molecular and crystal orbitals in finite and extended hydrocarbons. We can also think about the generation of bands from the following view points: In the series methane, ethane, propane, butane, ..., polyethylene, the number of orbitals increases with molecular size, leading to a correspondingly smaller separation between the orbital energy levels.[58] Drawing a continuous band is then an idealized repre-

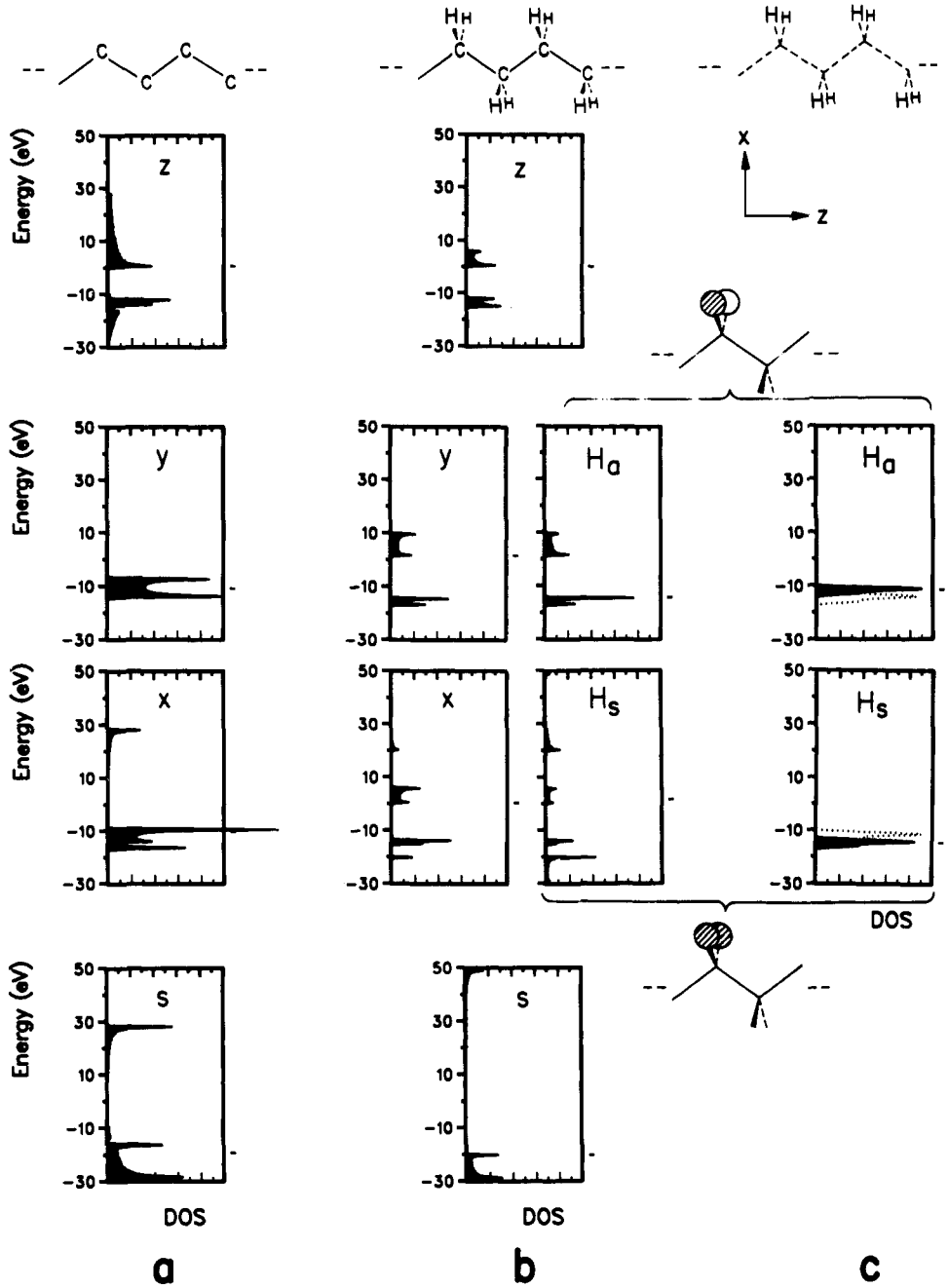

Figure 22. Projected DOS plots for the orbitals of polyethylene (b) and its carbon (a) and hydrogen fragment (c) (shaded areas, magnified 2×, except for (c)). The energy of half-filling for each projected orbital band is marked at the right-hand side of each DOS panel. The symmetric (H_s) and antisymmetric (H_a) linear combinations of the hydrogen orbitals have been projected out separately in (b) and (c) to better illustrate their respective interactions with the C x and C y orbitals, respectively, of the same symmetry. Note the matching x/H_s or y/H_a peak positions in the projections in (b). In (c) the total DOS (dotted line) is included to facilitate a comparison with the band structure in Figure 20c.

sentation for a large number of very close energy levels of the same type.

Electronic Spectra

In the following we will show briefly that band structure diagrams and density of state plots are observables, which may be probed by photelectron spectroscopy.

Figure 25 illustrates the mapping of the filled valence band of hexatriacontane, n-$CH_3(CH_2)_{34}CH_3$, over the whole Brillouin zone, by angle-resolved ultraviolet photoelectron spectroscopy (ARUPS).[22] This may be compared to our band structure diagrams in Figures 20 and 21. Figure 26 compares the calculated density of states for the filled levels of polyethylene with its XPS spectrum.

The reader may notice that the experimental spectra given here cover only filled levels. This is an inherent feature of the photoemission methods employed, which provide only information on filled bands. Information about the conduction bands can be obtained from secondary electron emission (SEE) spectra and inverse photoemission studies. However, here the correlation to the calculated DOS for polyethylene has not been well established.[25-28]

Comparing Polyacetylene and Polyethylene

In what follows, we compare the band structures of polyacetylene and polyethylene directly, showing their relationship by pinpointing the essential change when going from one to the other, while underscoring their similarity.

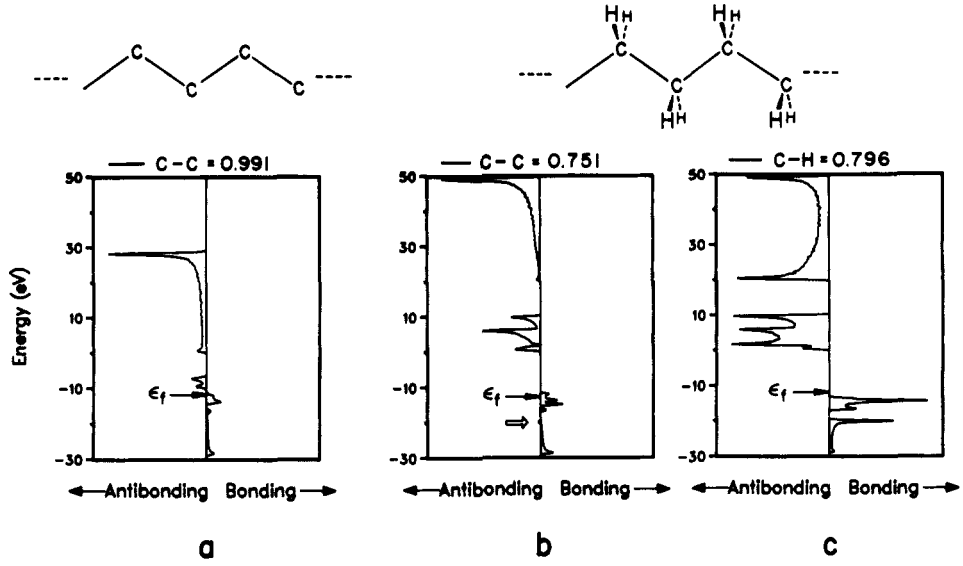

Figure 23. COOP plot for polyethylene illustrating the C–C (b) and C–H (c) bonding character of the bands, contrasted to the COOP for the carbon backbone (a) (C–C 154 pm). The given Fermi level and overlap populations are for the normal 12 electrons per unit cell.

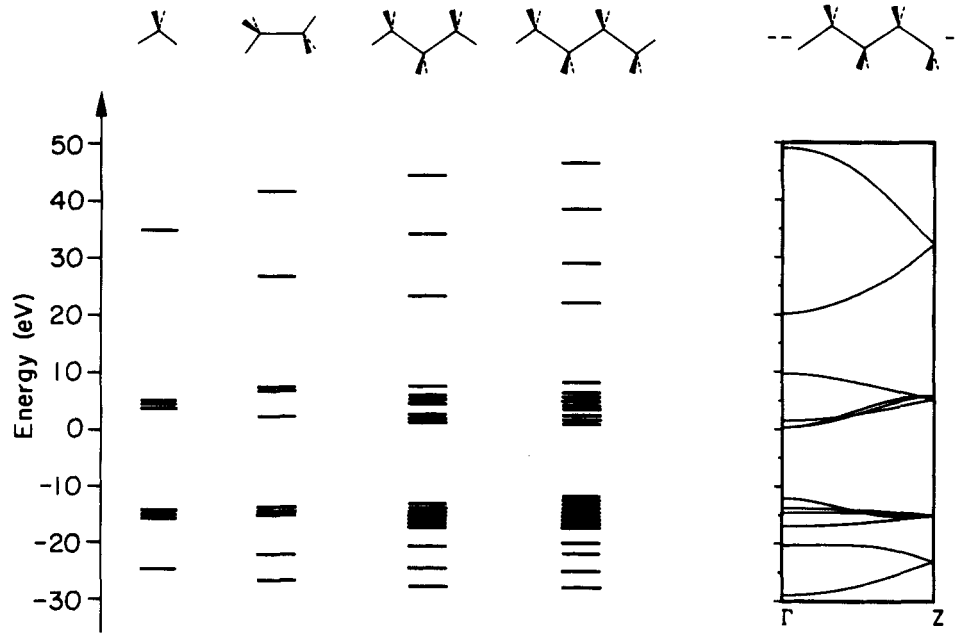

Figure 24. Distribution of orbital levels going from methane to polyethylene (cf. Figure 1 in ref 58b).

It is pretty simple. One can say that the two π_y bands of polyacetylene are replaced by a filled, y-H bonding, and an empty, y-H antibonding, combination in polyethylene (cf. Figure 21). Figure 27 shows this interaction of the polyacetylene π_y band with the antisymmetric hydrogen combination bringing about the large band gap in polyethylene in a "natural way".

The qualitative features of the rest of the band structure are surprisingly similar for polyacetylene and polyethylene (with the symmetric combination of hydrogen orbitals in the latter replacing the single hydrogen atom in the former). This similarity is demonstrated in Figure 28, comparing the band structure for polyethylene to symmetric polyacetylene, with the carbon y bands artificially removed in the two cases. The differences are due to the shorter C–C bond length in polyacetylene, the slightly different extent of carbon backbone kinking, and also, of course, to the different positions of the H atoms.

Some additional points can be made about C–C bond strength, bond alternation (polyacetylene) or its absence (polyethylene), and the conformation flexibility of the saturated chain.

Consider the starting point of the linear C chain. In this case, no antibonding levels are present below the Fermi level. This is because the π bands are just half-filled (13) with the states at the Fermi level being nonbonding, just at the transition from bonding to antibonding. Not very much changes for the kinked C chain. In polyacetylene, on the other hand, due to the bonding interaction with the hydrogens, one of the former π bands, the x band, is pushed completely below the Fermi level (see diagram 17) and with it of course, also its C–C antibonding upper half (σ_{CH_2} in 17), which had been empty before. The y band remains half-filled, its C–C antibonding levels therefore being empty. In polyethylene, in addition to the x band, the y band is also pushed below the Fermi level. Thus, its C–C antibonding levels are filled up, thereby further weakening C–C bonding. The lack of stabilization by the conjugated system, localized or not, reduces the stability of the all-planar carbon backbone conformation of polyethylene.

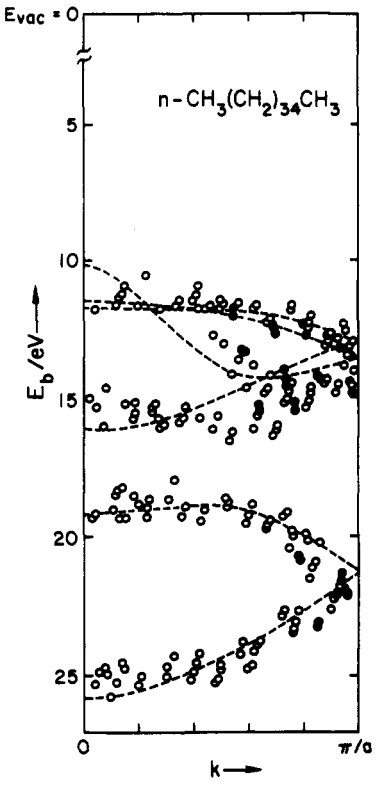

Figure 25. Valence band map of hexatriacontane (n-$CH_3(CH_2)_{34}$-CH_3, a model substance for polyethylene) as obtained by angle-resolved ultraviolet photoelectron spectroscopy (ARUPS). The experimental results are indicated by open and filled circles. An ab initio calculated band structure for polyethylene is drawn in with dashed lines. Reprinted with permission from ref 22. Copyright 1987 Elsevier Science Publishers. Note: Binding energy, E_b, is plotted here as the ordinate, hence the positive energy values. Compare to our results in Figures 20b and 21; valence band interval from −30 to −10 eV.

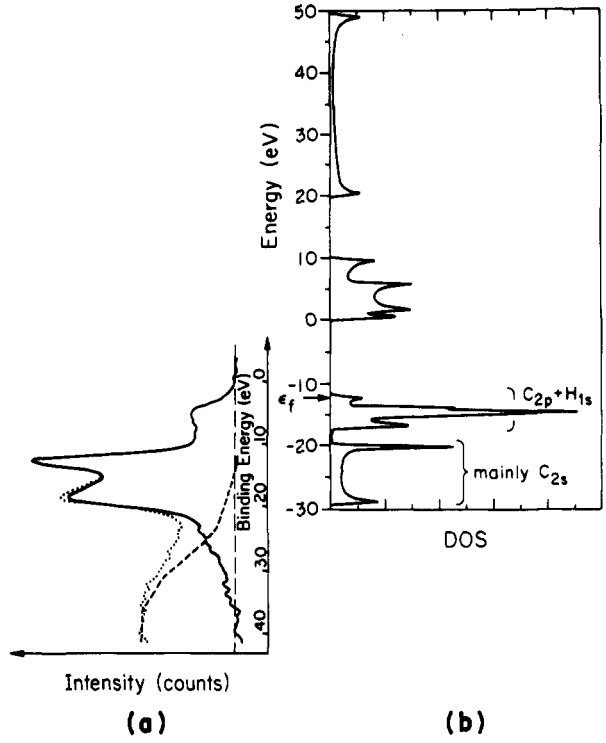

Figure 26. (a) Electron distribution curve for the valence region of polyethylene recorded from XPS/ESCA measurements: noise curve (dashed line), experimental curve (dotted line), corrected curve (solid line). Reprinted with permission from ref 17. Copyright 1974 American Institute of Physics. (b) Calculated total DOS for polyethylene (filled and unfilled levels). The lowest energy band (−30 to −20 eV) consists of mainly C_{2s}, the next high energy part (−17 to −12 eV) is C_{2p} and H_{1s} in character (cf. Figure 22b). In view of the larger photoionization cross section of C_{2s} electrons compared with that of p electrons, peak II is expected to be more intense than peak I in a.

Upon substitution one in fact observes a variety of helical conformations.[59]

As for bond alternation—that is a consequence of a half-filled band, a Peierls distortion. In the case of the carbon chain and of polyacetylene one has two and one, respectively, such half-filled bands. In polyethylene one has a large band gap, therefore no incentive for distortion. It is interesting how chemical and physical viewpoints converge on the same reality. Our language may differ, but the molecule remains the same.

Different Geometries, More Complicated Unit Cells

The *all-trans*-polyacetylene, and the *all-trans*-polyethylene, are of course idealized crystalline orientations of these polymers. Other regular conformations, not to speak of random chains, exist. What complications ensue?

To examine a simple case let us take a possible *cis-trans*-polyethylene **28**. Its unit cell obviously contains

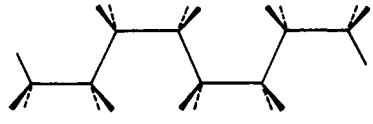

28

four CH_2 units vs two for the normal *all-trans*-polyethylene. And it will be less stable, because of the eclipsing of some bonds and 1,4 hydrogen interactions. But at the fundamental level of C–C and C–H bonding this is still polyethylene.

Let us see how the band structure reflects the chemical similarities and differences in *all-trans*- and *cis-trans*-polyethylene. Their levels are compared in Figure 29.[20,60]

Note that the Brillouin zone is halved (four CH_2's per repeat unit instead of two). So there are twice as many bands in the cis–trans polymer. There is still a degeneracy at the zone edge, due to the 2_1 screw axis. The bands are in approximately the same energy region in the two conformations of polyethylene.

There is a slight destabilization of the cis–trans polymer, which we can calculate. The cis–trans polymer is 31.5 kJ/mol per CH_2 unit less stable than *all-trans*-polyethylene.

The band structure emphasizes the differences. But underneath these are very similar conformations of one and the same polymer, $(CH_2)_n$, a molecule that contains C–C and C–H localized bonds. The DOS and COOP curves (not presented here) confirm this viewpoint—they are nearly identical. There are small differences, as there should be, between the two distinct C–C bonds in the cis–trans form. But these are minor.

What we have seen is a general phenomenon. Enlarging the unit cell will create more orbitals per unit cell, therefore more bands. But nothing will change fundamentally in the electron distribution or bonding.

Of course, if parts of a molecule bump into other parts, there cannot be any advantage to that. Steric effects count; in fact, they are determinative of much of polymer structure. How do they enter into our calculations? At the simple one-electron level, which is where the extended

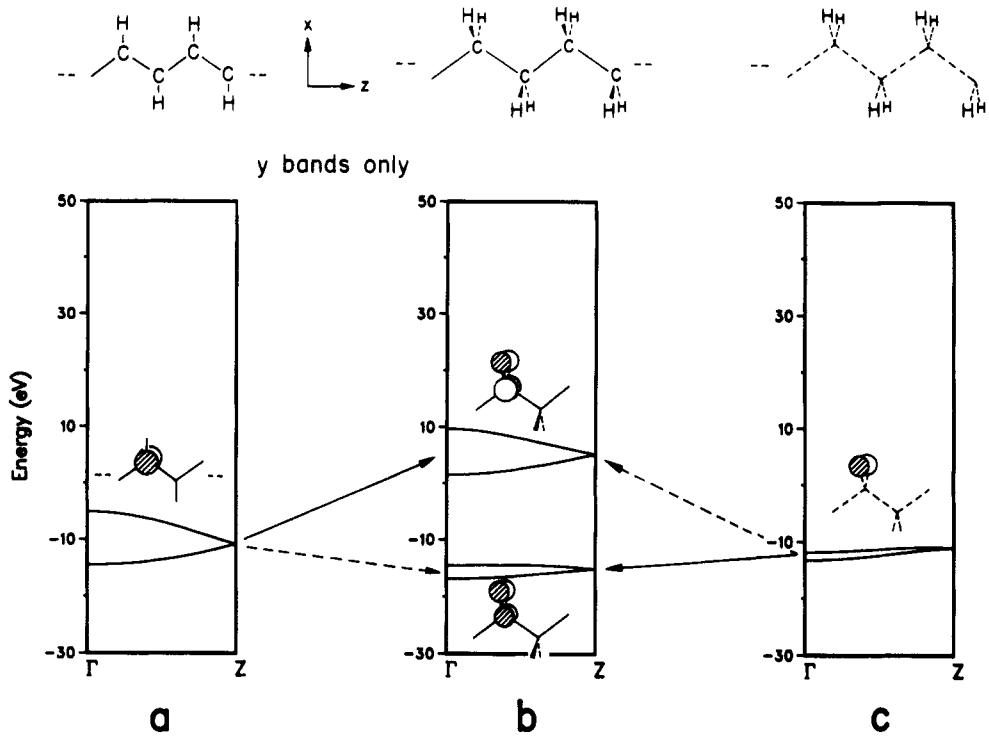

Figure 27. "Interaction" of the polyacetylene π_y band (no bond alternation, a) with the antisymmetric hydrogen combination (c), giving the polyethylene C y-H bands (b) and opening up a large band gap. The bonding combination in (b) is more hydrogen in character, the antibonding bands more carbon y, as indicated by the solid and dashed arrows (cf. projected DOS in Figure 22b). The C–C distances are those seen before: 140 pm for polyacetylene, 154 pm for polyethylene.

Hückel method is positioned, these enter through the four-electron two-orbital interaction. The idea is the following: If we have two-electron two-orbital interactions (**29a**), they are perforce bonding. If we add two more electrons (**29b**), we get net antibonding.

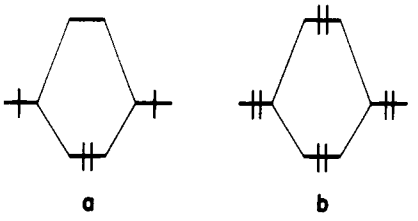

29

This is what happens in He_2, or to the lone pairs of two ammonias, were we inclined to push those lone pairs onto each other. And it is what happens if we push two filled C–H bonding orbitals onto each other (**30**) past their van der Waals minimum, so that the hydrogens are forced to approach to a distance less than ~210 pm of each other.

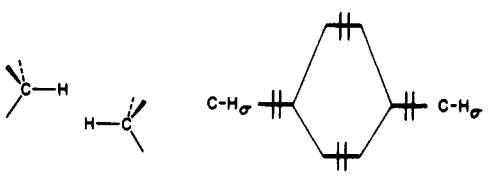

30

As we said, steric effects are determinative of the structure of most polymers. At least they serve to rule out large regions of any conformational diagram.[61]

Fine tuning of structure within sterically allowed regions occurs through conjugative and hydrogen-bonding interactions, where those are available.

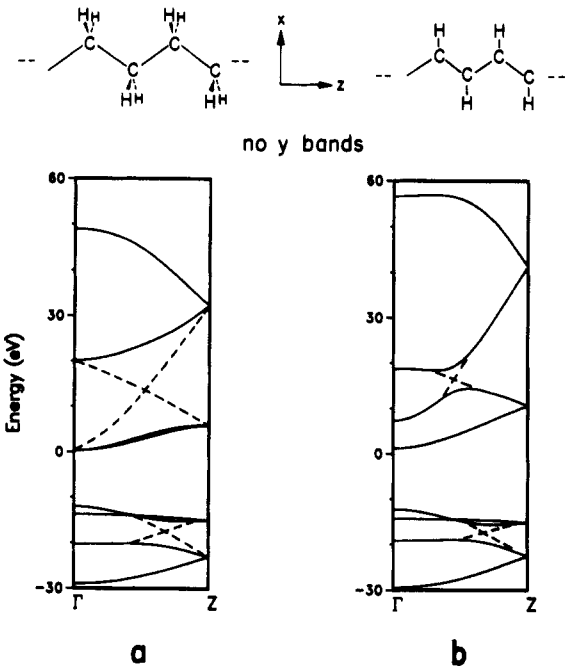

Figure 28. Band structures of polyethylene (a) and *all-trans*-polyacetylene (b) with equal bond lengths. The y bands have been removed to show the similarities in the σ-symmetrical bands (cf. Figures 13b, 15, and 20b). Dashed lines represent avoided crossings. C–C distances and angles were left unchanged from values given previously: 154 pm, tetrahedral in (a); 140 pm, 120° in (b).

Though much work of others is available on polymer conformations, which we do not mean to slight, we want to illustrate this steric control of conformation by an example drawn from our recent work.[62] The polymer in question is the relatively exotic polyisocyanide (**31**). It exists, for large R, as a 4-fold helix, as shown.

The helical symmetry is actually very useful for classifying the levels even of planar polymers.[59] One can define

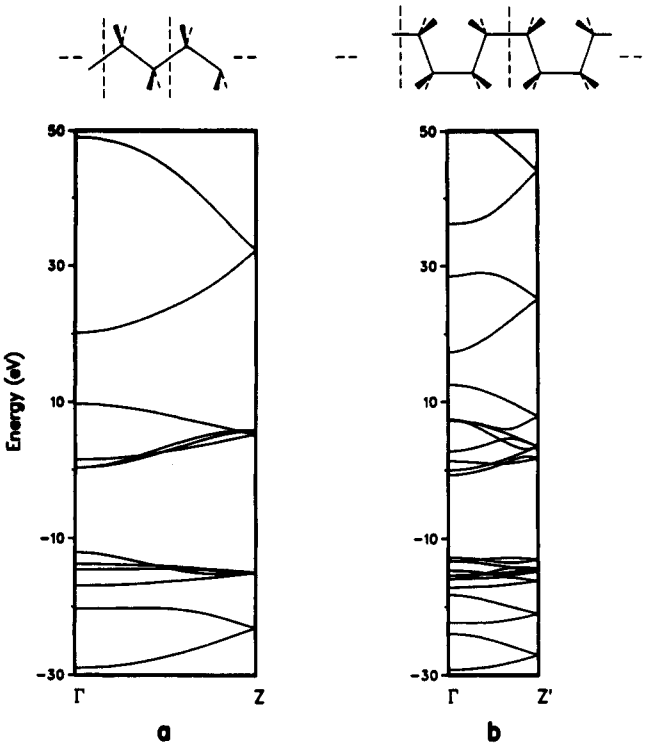

Figure 29. Differences and similarities between *all-trans*-(a) and *cis–trans*-(b) polyethylene as reflected in the band structure. The band structure of (b) contains twice as many bands (crystal orbitals) as (a) due to the doubled unit cell (halved Brillouin zone).

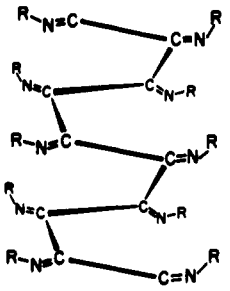

31

a helix angle θ, as in **32**. Thus the *all-trans*-polyethylene would have $\theta = 180°$, the 4-fold helix of RNC $\theta = 90°$.

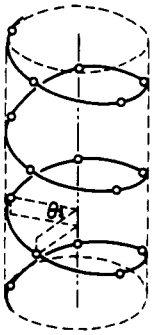

32

In Figure 30 we show the total energy of an RNC polymer as a function of R. Note the very broad range of available geometries for the hypothetical R = H chain. In that case the all-planar geometry ($\theta = 180°$) is slightly disfavored, for reasons given in our paper.[62] As R increases in size, the available region of phase space narrows. Note the very sharp conformational minimum at $\theta \approx 90°$ for R = *tert*-butyl, a polymer that is real. For R = methyl, an intermediate case, the energy well for the $\theta = 90°$ helix is already well developed. The second, separate helix minimum is an intriguing prediction.

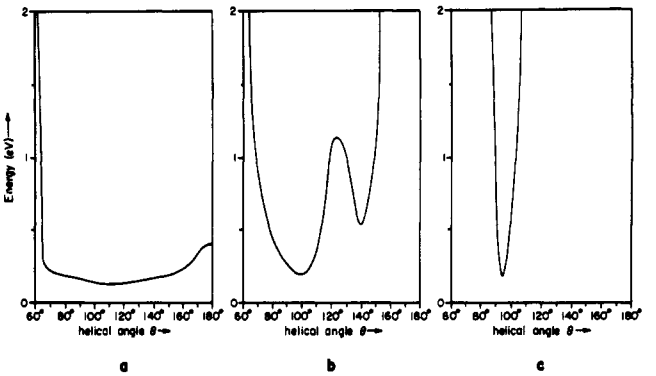

Figure 30. Total energy per unit cell as a function of the helical angle θ in polyisocyanides, $(RNC)_\infty$, with R = H (a), R = CH_3 (b), and R = $C(CH_3)_3$ (c). There is a common arbitrary energy zero.

Acknowledgment. We thank the Deutsche Forschungsgemeinschaft (DFG) for the award of postdoctoral fellowships for C.J. and C.K. and the National Science Foundation for its generous support through Grant CHE-8912070. This work was also supported by the Office of Naval Research. We are grateful to Jane Jorgensen and Elisabeth Fields for their expert drawings.

Appendix

The computations were performed within the extended Hückel formalism[35] with weighted H_{ij}'s.[63] The following atomic parameters were used in the calculations (H_{ii}, orbital energy; ζ, Slater exponent): C 2s, −21.4 eV, 1.63; 2p, −11.4 eV, 1.63; H 1s, −13.6 eV, 1.3.[35] Geometrical parameters such as C–C distances and C–C–C angles are referred to in the text or in figure captions; the C–H distance was fixed at 110 pm for both polyethylene and polyacetylene. A 100*k* point set was typically used for the average property calculations (DOS, COOP).

References and Notes

(1) See, for example: Alper, J.; Nelson, G. L. *Polymeric Materials*; American Chemical Society: Washington, DC, 1989; and references therein.
(2) *Chem. Eng. News* **1989**, *67* (Dec 11), 26.
(3) Ward, I. M. Key Polymers, Properties and Performance. *Adv. Polym. Sci.* **1985**, *70*, 1.
(4) (a) Skotheim, T. A., Ed. *Handbook of Conducting Polymers*; Marcel Dekker: New York, 1986; Vols. 1 and 2. (b) Billingham, N. C.; Calvert, P. D. Conducting Polymers/Molecular Recognition. *Adv. Polym. Sci.* **1989**, *90*, 1.
(5) Kroschwitz, J. I., Ed. *Electrical and Electronic Properties of Polymers*; Encyclopedia Reprint Series; Wiley: New York, 1988.
(6) (a) Fisher, A. J.; Hayes, W.; Wallace, D. S. *J. Phys.: Condens. Matter* **1989**, *1*, 5567. (b) Rice, M. J.; Phillpot, S. R.; Bishop, A. R.; Campbell, D. K. *Phys. Rev. B* **1986**, *34*, 4139.
(7) (a) Su, W. P.; Schrieffer, J. R.; Heeger, A. J. *Phys. Rev. Lett.* **1979**, *42*, 1698. (b) Su, W. P.; Schrieffer, J. R.; Heeger, A. J. *Phys. Rev. B* **1980**, *22*, 2099.
(8) (a) Brédas, J. L. *Mol. Cryst. Liq. Cryst.* **1985**, *118*, 49. (b) Brédas, J. L.; Chance, R. R.; Silbey, R. *Phys. Rev. B* **1982**, *26*, 5843. (c) Brédas, J. L.; Thémans, B.; André, J. M. *Phys. Rev. B* **1983**, *27*, 7827; see also ref 4.
(9) Sinclair, M.; Moses, D.; Akagi, K.; Heeger, A. J. *Phys. Rev. B* **1988**, *38*, 10724, and references therein.
(10) (a) Naarmann, H.; Theophilou, N. *Synth. Met.* **1987**, *22*, 1. (b) Naarmann, H. In *Electronic Properties of Conjugated Polymers II*; Kuzmany, H., Mehring, M., Roth, S., Eds.; Springer Series in Solid-State Sciences; Springer-Verlag: Berlin, 1987; Vol. 76, p 12. (c) Tsukamoto, J.; Takahashi, A.; Kawasaki, K. *Jpn. J. Appl. Phys.* **1990**, *19*, 125.
(11) (a) Akagi, K.; Suezaki, M.; Shirakawa, H.; Kyotani, H.; Shimomura, M.; Tanabe, Y. *Synth. Met.* **1989**, *28*, D1. (b) For a

clear recent discussion of the Young's modulus of polyacetylene as a function of doping, see: Hong, S. Y.; Kertesz, M. *Phys. Rev. Lett.* **1990**, *64*, 3031.
(12) See, however: Sixl, H. In *Electronic Properties of Conjugated Polymers III*; Kuzmany, H., Mehring, M., Roth, S., Eds.; Springer Series in Solid-State Sciences; Springer-Verlag: Berlin 1989; Vol. 91, p 477.
(13) Chien, J. C. W. *Polyacetylene—Chemistry, Physics, and Material Science*; Academic Press: New York, 1984.
(14) (a) Yang, X. Q.; Tanner, D. B.; Rice, M. J.; Gibson, H. W.; Feldblum, A.; Epstein, A. J. *Solid State Commun.* **1987**, *61*, 335. (b) Chung, T. C.; Moraes, F.; Flood, J. D.; Heeger, A. J. *Phys. Rev. B* **1984**, 29, 2341.
(15) For a list of references about calculations on polyethylene at different levels of sophistication, see refs 16 and 17, and for critical comparisons on the different levels of band structure calculations on polyethylene, see refs 18–20.
(16) (a) Springborg, M.; Lev, M. *Phys. Rev. B* **1989**, *40*, 3333. (b) André, J. M. In *Electronic Structure of Polymers and Molecular Crystals*; André, J. M., Ladik, J., Eds.; Plenum Press: New York, 1975; p 1; for list see p 16.
(17) Delhalle, J.; André, J. M.; Delhalle, S.; Pireaux, J. J.; Caudano, R.; Verbist, J. J. *J. Chem. Phys.* **1974**, *60*, 595.
(18) Seki, K.; Ueno, N.; Karlsson, U. O.; Engelhardt, R.; Koch, E.-E. *Chem. Phys.* **1986**, *105*, 247.
(19) Karpfen, A. *J. Chem. Phys.* **1981**, *75*, 238.
(20) André, J. M. *Adv. Quantum Chem.* **1980**, *12*, 65.
(21) (a) Seki, K.; Inokuchi, H. *Chem. Phys. Lett.* **1982**, *89*, 268. (b) Seki, K.; Hashimoto, S.; Sato, N.; Harada, Y.; Ishii, K.; Inokuchi, H.; Kanbe, J.-I. *J. Chem. Phys.* **1977**, *66*, 3644.
(22) Fujimoto, H.; Mori, T.; Inokuchi, H.; Ueno, N.; Sugita, K.; Seki, K. *Chem. Phys. Lett.* **1987**, *141*, 485.
(23) Clark, D. T. In *Electronic Structure of Polymers and Molecular Crystals*; André, J. M., Ladik, J., Eds.; Plenum Press: New York, 1975, p. 259.
(24) (a) Pireaux, J. J.; Caudano, R.; Verbist, J. *J. Electron Spectrosc. Relat. Phenom.* **1974**, *5*, 267. (b) Wood, M. H.; Barber, M.; Hillier, I. H.; Thomas, J. M. *J. Chem. Phys.* **1972**, *56*, 1788.
(25) Ueno, N.; Sugita, K.; Kiyono, S. *Chem. Phys. Lett.* **1981**, *82*, 296.
(26) Ueno, N.; Fukushima, T.; Sugita, K.; Kiyono, S.; Seki, K.; Inokuchi, H. *J. Phys. Soc. Jpn.* **1980**, *48*, 1254.
(27) Ueno, N.; Sugita, K. *Solid State Commun.* **1980**, *34*, 355.
(28) Ueno, N.; Sugita, K. *Jpn. J. Appl. Phys.* **1979**, *18*, 2159.
(29) Ritsko, J. J. *J. Chem. Phys.* **1979**, *70*, 5343.
(30) Less, K. J.; Wilson, E. G. *J. Phys. C* **1973**, *6*, 3110.
(31) Kitani, I.; Yoshimo, K.; Inuishi, Y. *Jpn. J. Appl. Phys.* **1980**, *19*, 765.
(32) (a) Springborg, M.; Kiess, H.; Hedegård, P. *Synth. Met.* **1989**, *31*, 281, and references therein. (b) Kertész, M. *Adv. Quantum Chem.* **1982**, *15*, 161, and references therein. (c) Karpfen, A. *Phys. Scr.* **1982**, *T1*, 79, and references therein.
(33) For approaches in the same spirit, see: (a) Albright, T. A.; Burdett, J. K.; Whangbo, M.-H. *Orbital Interactions in Chemistry*; Wiley-Interscience: New York, 1985; Chapter 20. (b) Burdett, J. K. *Prog. Solid State Chem.* **1984**, *15*, 173. (c) Whangbo, M.-H. In *Extended Linear Chain Compounds*; Miller, J. S., Ed.; Plenum Press: New York, 1982; p 127. (d) Gerstein, B. C. *J. Chem. Educ.* **1973**, *50*, 316. (e) Lowe, J. P.; Kafafi, S. A.; LaFemina, J. P. *J. Phys. Chem.* **1986**, *90*, 6602. (f) Brus, L. *Nouv. J. Chim.* **1987**, *11*, 123.
(34) Although in one case Seki et al.[21b] also pointed out that a calculation on an isolated chain is insufficient. For an accurate position of the conduction band, for example, it is necessary to consider the interchain interaction, because the excited electron moves to other molecules even in its lowest excited state.
(35) (a) Hoffmann, R. *J. Chem. Phys.* **1963**, *39*, 1397. (b) Hoffmann, R.; Lipscomb, W. N. *J. Chem. Phys.* **1962**, *37*, 2872; *36*, 2179.
(36) McCubbin, W. L.; Manne, R. *Chem. Phys. Lett.* **1968**, *2*, 230.
(37) A somewhat similar approach has been taken in the construction of the band structures for some ring and ladder polymers by Lowe et al.[33e]
(38) Hoffmann, R.; Fujimoto, H.; Swenson, J. R.; Wan, C.-C. *J. Am. Chem. Soc.* **1973**, *95*, 7644.
(39) Hoffmann, R.; Fujimoto, H. *J. Phys. Chem.* **1974**, *78*, 1167.
(40) Weltner, W., Jr.; van Zee, R. J. *Chem. Rev.* **1989**, *89*, 1713.
(41) (a) Curl, R. F.; Smalley, R. E. *Science* **1988**, *242*, 30. (b) Parent, D. C.; McElvany, S. W. *J. Am. Chem. Soc.* **1989**, *111*, 2393.
(42) Akagi, K.; Nishiguhi, M.; Shirakawa, H.; Furukawa, Y.; Harada, I. *Synth. Met.* **1987**, *17*, 557.
(43) Ashcroft, N. W.; Mermin, N. D. *Solid State Physics*; Saunders: Philadelphia, PA, 1976.
(44) A thermodynamic definition of the Fermi level, especially important for semiconductors, places it between the highest occupied and the lowest unoccupied levels.
(45) Mulliken, R. S. *J. Chem. Phys.* **1955**, *23*, 1833, 2343.
(46) (a) Dedieu, A.; Hoffmann, R. *J. Am. Chem. Soc.* **1978**, *100*, 2074. (b) Mehrotra, P. K.; Hoffmann, R. *Inorg. Chem.* **1978**, *17*, 2187. (c) Merz, K. M., Jr.; Hoffmann, R. *Inorg. Chem.* **1988**, *27*, 2120.
(47) (a) Melnitchenko, V. M.; Smirnov, B. N.; Varlakov, V. P.; Nikulin, Yu. N.; Sladkov, A. M. *Carbon* **1983**, *21*, 131. (b) Kasatochkin, V. I.; Korshak, V. V.; Kudryavtsev, Yu. P.; Sladkov, A. M.; Sterenberg, I. E. *Carbon* **1973**, *11*, 70, and references therein.
(48) (a) Karpfen, A. *J. Phys. C* **1979**, *12*, 3227. (b) Kertesz, M.; Koller, J.; Azman, A. *J. Chem. Phys.* **1978**, *68*, 2779. (c) For an early discussion of C_n chains, see: Hoffmann, R. *Tetrahedron* **1966**, *22*, 521.
(49) Longuet-Higgins, H. C.; Salem, L. *Proc. R. Soc. London* **1959**, *A251*, 172.
(50) (a) Yannoni, C. S.; Clarke, T. C. *Phys. Rev. Lett.* **1983**, *51*, 1191. (b) Fincher, C. R., Jr.; Chen, C. E.; Heeger, A. J.; MacDiarmid, A. G.; Hastings, J. B. *Phys. Rev. Lett.* **1982**, *48*, 100. (c) Shimamura, K.; Karasz, F. E.; Hirsch, J. A.; Chien, J. C. W. *Makromol. Chem., Rapid Commun.* **1981**, *2*, 473. (d) Lieser, G.; Wegner, G.; Müller, W.; Enkelmann, V.; Meyer, W. H. *Makromol. Chem., Rapid Commun.* **1980**, *1*, 627.
(51) (a) Peierls, R. E. *Quantum Theory of Solids*; Oxford University Press: London, 1955; p 108. (b) Whangbo, M.-H. *Crystal Chemistry and Properties of Materials with Quasi-One-Dimensional Structures*; Rouxel, J., Ed.; D. Reidel: Dordrecht, The Netherlands, 1986; p 27. (c) Roth, S. *Synth. Met.* **1989**, *34*, 617. (d) Kertesz, M.; Koller, J.; Azman, A. *J. Chem. Phys.* **1977**, *67*, 1180. (e) Whangbo, M.-H.; Hoffmann, R.; Woodward, R. B. *Proc. R. Soc. London* **1979**, *A366*, 23.
(52) (a) Jahn, H. A.; Teller, E. *Proc. R. Soc. London* **1937**, *A161*, 220. (b) Englman, R. *The Jahn–Teller Effect in Molecules and Crystals*; Wiley-Interscience: New York, 1972. (c) Stoneham, A. M. *Theory of Defects in Solids*; Clarendon Press: Oxford, U. K., 1975. (d) Bersuker, I. B. *The Jahn–Teller Effect: A Bibliographical Review*; Plenum: New York, 1984. (e) Bersuker, I. B. *The Jahn–Teller Effect and Vibronic Interactions in Modern Chemistry*; Plenum: New York, 1984.
(53) Pople, J. A.; Walmsley, S. H. *Mol. Phys.* **1962**, *5*, 15. For leading references to the way the discussion has moved since then, see: König, G.; Stollhoff, G. *Phys. Rev. Lett.* **1990**, *65*, 1239.
(54) See the discussion: Charge Transfer in Polymeric Systems. *Faraday Discuss. Chem. Soc.* 1989, *No. 88*.
(55) Actually, the situation is more complicated with the occurrence of negative radical electron spin densities due to electron correlation effects, but that is beyond the scope of our one-electron picture.
(56) Polyethylene: (a) Iohara, K.; Imada, K.; Tagayanagi, M. *Polym. J.* **1972**, *3*, 354. (b) Kavesh, S.; Schultz, J. M. *J. Polym. Sci. A* **1970**, *8*, 243. (c) Bunn, C. W. *Trans. Faraday Soc.* **1939**, *35*, 482. *n*-Hexatriacontane, $C_{36}H_{74}$: (d) Teare, P. W. *Acta Crystallogr.* **1959**, *12*, 294. (e) Shearer, H. M. M.; Vand, V. *Acta Crystallogr.* **1956**, *9*, 379. (f) Avitabile, G.; Napolitano, R.; Pirozzi, B.; Rouse, K. D.; Thomas, M. W.; Willis, B. T. M. *J. Polym. Sci., Polym. Lett.* **1975**, *13*, 351.
(57) We could, of course, make use of the screw axis or glide plane along the chain direction, thereby reducing the unit cell to a single methylene group and unfolding the bands—a procedure opposite to the folding sketched in Figure 10.
(58) (a) Huckel, E. *Z. Phys.* **1932**, *76*, 626. (b) André, J. M.; Delhalle, J. *Quantum Theory of Polymers*; André, J. M., Delhalle, J., Ladik, J., Eds.; Proceedings, NATO ASI on Electronic Structure and Properties of Polymers, D. Reidel: Dordrecht, The Netherlands, 1978; p 1. (c) Cui, C. X.; Kertesz, M.; Jiang, Y. *J. Phys. Chem.* **1990**, *94*, 5172.
(59) (a) Cui, C. X.; Kertesz, M. *J. Am. Chem. Soc.* **1989**, *111*, 4216. (b) Cui, C. X.; Kertesz, M. In *Electronic Properties of Conjugated Polymers III*; Kuzmany, H., Mehring, M., Roth, S., Eds.; Springer Series in Solid-State Sciences; Springer-Verlag: Berlin, 1989; Vol. 91, p 73.
(60) (a) see also: Delhalle, J.; André J. M.; Delhalle, S.; Pivont-Malherbe, C.; Clarisse, F.; Leroy, G.; Peeters, D. *Theor. Chim. Acta* **1977**, *43*, 215. (b) The cis–trans problem in polyacetylene is discussed, inter alia, in ref 51e.
(61) Nemethy, G.; Scheraga, H. A. *Q. Rev. Biophys.* **1977**, *10*, 239, and references therein.
(62) Kollmar, C.; Hoffmann, R. *J. Am. Chem. Soc.* **1990**, *112*, 8230. See also: Cui, C.-X.; Kertesz, M. *Chem. Phys. Lett.* **1990**, *169*, 445.
(63) Ammeter, J. H.; Bürgi, H.-B.; Thibeault, J. C.; Hoffmann, R. *J. Am. Chem. Soc.* **1978**, *100*, 3686.

Registry No. *n*-$CH_3(CH_2)_{34}CH_3$, 630-06-8; *trans*-poly(acetylene) (SRU), 25768-71-2; polyethylene (homopolymer), 9002-88-4.